View metadata, citation and similar papers at core.ac.uk

brought to you by CORE

provided by IntechOpen

We are IntechOpen, the world's leading publisher of Open Access books Built by scientists, for scientists

4,800
Open access books available

122,000
International authors and editors

135M
Downloads

Our authors are among the

154
Countries delivered to

TOP 1%
most cited scientists

12.2%
Contributors from top 500 universities

CLARIVATE ANALYTICS BOOK CITATION INDEX INDEXED

WEB OF SCIENCE™

Selection of our books indexed in the Book Citation Index in Web of Science™ Core Collection (BKCI)

Interested in publishing with us?
Contact book.department@intechopen.com

Numbers displayed above are based on latest data collected.
For more information visit www.intechopen.com

12

Quantum Information-Theoretical Analyses of Systems and Processes of Chemical and Nanotechnological Interest

Rodolfo O. Esquivel[1,5] et al.[*]
[1]*Departamento de Química, Universidad Autónoma Metropolitana-Iztapalapa, México D.F.*
[5]*Instituto Carlos I de Física Teórica y Computacional, Universidad de Granada, Granada*
[1]*México*
[5]*Spain*

1. Introduction

The application of information-theoretic concepts and techniques to the study of quantum multielectronic systems is presently attracting the attention of numerous researchers in several fields. This area of inquiry is shedding new light on the conceptual foundations of physics and is also at the core of the new field of Quantum Information Theory, which foresees important technological developments through concepts such as "entanglement", "teleportation" and "quantum computation". In line with these developments we present in this Chapter a review of the recent advances performed in our laboratories to study selected molecular processes and mesoscopic systems at the nanoscopic scale by employing information theory concepts to show significant advances of Information Theory applied to chemistry by use of Shannon entropies through the localized/delocalized features of the electron distributions allowing a phenomenological description of the course of elementary chemical reactions by revealing important chemical regions that are not present in the energy profile such as the ones in which bond forming and bond breaking occur. Further, the synchronous reaction mechanism of a S_N2 type chemical reaction and the non-synchronous mechanistic behavior of the simplest hydrogenic abstraction reaction were predicted by use of Shannon entropies analysis. These studies have shown that the information-theoretical measures provide evidence to support the concept of a continuum of transient of Zewail and Polanyi for the transition state rather than a single state, which is also in agreement with other analyses. Although information entropies have been employed in quantum chemistry, applications in large chemical systems are very scarce. For nanostructures, we have been able to show that IT measures can be successfully employed

[*] Edmundo M. Carrera[1], Cristina Iuga[1], Moyocoyani Molina-Espíritu[1], Juan Carlos Angulo[2,5], Jesús S. Dehesa[2,5], Sheila López-Rosa[2,5], Juan Antolín[3,5] and Catalina Soriano-Correa[4]
[1]*Departamento de Química, Universidad Autónoma Metropolitana-Iztapalapa, México D.F., México*
[2]*Departamento de Física Atómica, Molecular y Nuclear, Universidad de Granada, Granada, Spain*
[3]*Departamento de Física Aplicada, EUITIZ, Universidad de Zaragoza, Zaragoza, Spain*
[4]*Laboratorio de Química Computacional-QFB. FES-Zaragoza-UNAM, Iztapalapa, México, DF, México*
[5]*Instituto Carlos I de Física Teórica y Computacional, Universidad de Granada, Granada, Spain*

to analyse the growing behaviour of PAMAM dendrimers supporting the dense-core model against the hollow-core one.

2. Essentials of information theory: Classical and quantum

Information theory of quantum many-body systems is at the borderline of the development of physical sciences, in which major areas of research are interconnected, i.e., physics, mathematics, chemistry, and biology. Therefore, there is an inherent interest for applying theoretic-information ideas and methodologies to chemical, mesoscopic and biological systems along with the processes they exert. In this Section we briefly present the theory of the two possible levels, classical (Shannon, Fisher, complexity, etc) and quantum (von Neumann and other entanglement measures). The theoretic-information analyses presented here have been scarcely considered in the literature until recently and reveal important reactivity aspects of elementary chemical reactions which are not accessible by other theoretical methodologies. Therefore, we present important concepts of Information Theory along with the natural atomic probabilities employed for the calculation of the entropies.

2.1 Shannon information theory

The uncertainty in a collection of possible observables A_i with corresponding probability distribution $p_i(A)$ is given by its Shannon entropy $H(A)$ (Shannon and Weaver, 1949):

$$H(A) = -\sum_i p_i(A) \ln p_i(A) \tag{1}$$

This measure is suitable for systems described by classical physics, and is useful to measure uncertainty of observables but it is not suitable for measuring uncertainty of the general state of a quantum system. It is the von Neumann entropy which is appropriate to measure uncertainty of quantum systems since it depends on the density matrix (see below).

Suppose that we have two sets of discrete events A_i and B_j with the corresponding probability distributions, $p_i(A)$ and $p_j(B)$. The relative entropy between these two distributions is defined as

$$H(A\|B) = -\sum_i p_i(A) \ln \frac{p_i(A)}{p_i(B)} \tag{2}$$

This function, also known as Kullback-Leibler entropy (Kullback and Leibler, 1951; Raju et al, 1990) is a measure of the ''distance'' between $p_i(A)$ and $p_j(B)$, even though, strictly speaking, it is not a mathematical metric since it fails to be symmetric:

$$H(A\|B) \neq H(B\|A) \tag{3}$$

Another important concept derived from relative entropy concerns the gathering of information. When one system learns something about another, their states become correlated. How correlated they are, or how much information they have about each other, can be quantified by the mutual information. The Shannon mutual information between two random variables A and B, having a joint probability distribution $p_{ij}(A,B)$ and marginal probability distributions

$$p_i(A) = \sum_j p_{ij}(A,B) \text{ and } p_j(B) = \sum_i p_{ji}(B,A) \tag{4}$$

is defined as

$$\begin{aligned} H(A:B) &= H(A) + H(B) - H(A,B) \\ &= \sum_{ij} p_{ij}(A,B) \ln \frac{p_{ij}(A,B)}{p_i(A) p_j(B)} \end{aligned} \tag{5}$$

where H(A,B) is the joint entropy defined as

$$H(A,B) = -\sum_{ij} p_{ij}(A,B) \ln p_{ij}(A,B) \tag{6}$$

which measures the uncertainty about the whole system *AB*.
The mutual information *H(A:B)* can be written in terms of the Shannon relative entropy. In this sense it represents a distance between the distribution *p(A,B)* and the product of the marginals $p(A) \times p(B)$ As such, it is intuitively clear that this is a good measure of correlations, since it shows how far a joint distribution is from the product one in which all the correlations have been removed, or alternatively, how distinguishable a correlated state is from a completely uncorrelated one. So we have

$$H(A:B) = H\left[p(AB) \| p(A) \times p(B) \right] \tag{7}$$

Suppose that we wish to know the probability of observing *B* if *A* has been observed. This is called a conditional probability and is given by

$$p_{ij}(A|B) = \frac{p_{ij}(A,B)}{p_j(B)} \text{ and } p_{ji}(B|A) = \frac{p_{ji}(B,A)}{p_i(A)} \tag{8}$$

Hence the conditional entropy is,

$$\begin{aligned} H(A|B) &= -\sum_{ij} p_{ij}(A,B) \ln \frac{p_{ij}(A,B)}{p_j(B)} \\ &= -\sum_{ij} p_{ij}(A,B) \ln p_{ij}(A|B) \end{aligned} \tag{9}$$

This quantity, being positive, tells us how uncertain we are about the value of *B* once we have learned about the value of *A*. Now the Shannon mutual information can be rewritten as

$$H(A:B) = H(A) - H(A|B) \tag{10}$$

and the joint entropy as

$$H(A,B) = H(B) + H(A|B) \tag{11}$$

Hence, the Shannon mutual information, measures the quantity of information conveyed about the random variable *A(p(B))* through measurements of the random variable *B(p(A))*.

Note also that, unlike the Shannon relative entropy, the Shannon mutual information is symmetric. Besides, according to the properties of the logarithmic functions (Jensen inequality) it can be established that entropy is a concave function, $-\sum p_i x_i \ln \sum p_i x_i \geq -\sum p_i x_i \ln x_i$ meaning that mixing probability distributions increases entropy, whereas the relative entropy is a convex function, $\sum x_i \ln\left(\sum x_i \Big/ \sum a_i\right) \leq \sum x_i \ln\left(x_i \Big/ a_i\right)$ i.e., mixing decreases the distance between states (less distinguishable).

The difference between classical and quantum entropies can be seen in the fact that quantum states are described by a density matrix ρ (and not just probability vectors). The density matrix is a positive semidefinite Hermitian matrix, whose trace is unity. An important class of density matrices is the idempotent one, i.e., $\rho = \rho^2$. The states these matrices represent are called pure states. When there is no uncertainty in the knowledge of the system its state is then pure. Another important concept is that of a composite quantum system, which is one that consists of a number of quantum subsystems. When those subsystems are entangled it is impossible to ascribe a definite state vector to any one of them, unless we deal with a bipartite composite system. The most often cited entangled system is the Einstein-Podolsky-Rosen state (EPR) (Einstein et al., 1935: Bell, 1987), which describes a pair of two photons. The composite system is described by $\Psi(1,2) = \dfrac{\left(\left|\uparrow(1)\right\rangle\left[\left|\downarrow(2)\right\rangle\right] - \left[\left|\uparrow(2)\right\rangle\right]\left[\left|\downarrow(1)\right\rangle\right]\right)}{\sqrt{2}}$ which represents the spin directions along the z axis that can either be up or down. We can immediately see that neither of the photons possesses a definite state vector, then if a measurement is made on one photon, let say in the up state, then the other photon will be in the down state. This "assignment" cannot be applied to a general composite system unless its general state is written in a diagonal decomposable form, which not only is mathematically convenient, but also gives a deeper insight into correlations between the two subsystems. According to quantum mechanics the state vector of a composite system, consisting of subsystems *A* and *B*, is represented by a vector belonging to the tensor product of the two Hilbert spaces $H_A \otimes H_B$. The general state of this system can be written as a linear superposition of products of individual states:

$$\Psi^{AB} = \sum_m \sum_n c_{mn} \xi_m(A) \psi_n(B) \tag{12}$$

Where $\{\xi_m(A)$; m=1 to *M*$\}$ and $\{\psi_n(B)$; n=1 to *N*$\}$ are the basis of the subsystems *A* and *B*, respectively. This state can always be decomposed in the Schmidt diagonal form:

$$\Psi^{AB} = \sum_l \lambda_l \chi_l(A) \varphi_l(B) \tag{13}$$

Where $\chi_l(A)$ and $\varphi_l(B)$ are orthonormal bases for *A* and *B*, respectively. Note that in this form the correlations between the two subsystems are completely revealed. If *A* is found in the state $\chi_p(A)$, for example, then the state of B is in the $\varphi_p(B)$ state. This is clearly a multistate generalization of the EPR-state mentioned earlier.

In order to understand the correlation between two subsystems in a joint pure state we point out that the reduced density matrices of both subsystems, written in the Schmidt

decomposed state above, are diagonal and have the same positive spectrum. In particular, the overall density matrix is given by

$$\rho = \sum_{nm} \lambda_n \lambda_m^* \; |\chi_n(A)\rangle\langle\chi_m(A)| \otimes |\phi_n(B)\rangle\langle\phi_m(B)| \tag{14}$$

whereas the reduced ones are

$$\begin{aligned} \rho_A &= \sum_n \langle\phi_n(B)|\rho|\phi_n(B)\rangle \\ &= \sum_m |\lambda_m|^2 \, |\chi_m(A)\rangle\langle\chi_m(A)| \end{aligned} \tag{15}$$

and in analogous way

$$\rho_B = \sum_n |\lambda_n|^2 \, |\phi_n(B)\rangle\langle\phi_n(B)| \tag{16}$$

It is important to note that a *N*-dimensional subsystem can then be entangled with no more than *N* orthogonal states of another one. Schmidt decomposition is, in general, not practical for more than two entangled subsystems since for say *n* entangled systems is uncertain to know at the same time a general state such that by observing the state of one of the subsystems we could instantaneously know the state of the other *n-1*. Clearly, involvement of *n*-subsystems complicates the analysis and produces an even greater mixture and uncertainty. The same reasoning applies to mixed states of two or more subsystems (i.e., states whose density operator is not idempotent), for which we cannot have the Schmidt decomposition in general.

When two subsystems become entangled, the composite state can be expressed as a superposition of the products of the corresponding Schmidt basis vectors. From Eq. (13) it follows that the ith vector of either subsystem has a probability of $|\lambda|^2$ associated with it. We are, therefore, uncertain about the state of each subsystem, the uncertainty being larger if the probabilities are evenly distributed. Since the uncertainty in the probability distribution is naturally described by the Shannon entropy, this classical measure can also be applied in quantum theory. In an entangled system this entropy is related to a single observable. The general state of a quantum system, is described by its density matrix ρ. Let the observables a_i and b_j, pertaining to the subsystems A and B, respectively, have a discrete and non degenerate spectrum, with probabilities $p_i(A)$ and $p_j(B)$ In addition, let the joint probability be $p_{ij}(A,B)$. Then

$$\begin{aligned} H(A) &= -\sum_i p_i(A) \ln p_i(A) \\ &= -\sum_{ij} p_{ij}(A,B) \ln \sum_j \; p_{ij}(A,B) \end{aligned} \tag{17}$$

and similarly for *H(B).*

An indication of correlation is that the sum of the uncertainties in the individual subsystems is greater than the uncertainty in the total state. Hence, the Shannon mutual information is a good indicator of how much the two given observables are correlated. However, this quantity, as it is inherently classical, describes the correlations between single observables only.

2.2 Quantum information theory

The quantity that is related to the correlations in the overall state as a whole is the von Neumann mutual information which depends on the density matrix. The von Neumann entropy (von Neumann, 1955), may be considered as the proper quantum analog of the Shannon entropy (Wehrl, 1978) for a system described by a density matrix ρ, and is defined as

$$S(\rho) = -Tr(\rho \ln \rho) \tag{18}$$

The Shannon entropy is equal to the von Neumann entropy only when it describes the uncertainties in the values of the observables that commute with the density matrix, i.e., if ρ is a mixed state composed of orthogonal quantum states, otherwise

$$S(\rho) \leq H(A) \tag{19}$$

where A is any observable of a system described by ρ. This means that there is more uncertainty in a single observable than in the whole of the state (Vedral, 2002).

Let ρ_A and ρ_B be the reduced density matrices of subsystems A and B, respectively, and let ρ be the matrix of a composite system, then the entropies of two subsystems are somewhat analogous to its classical counterpart, but instead of referring to observables it is related to the two states which are bounded by the following Araki-Lieb (1970) inequality

$$S(\rho_A) + S(\rho_B) \geq S(\rho) \geq \left| S(\rho_A) - S(\rho_B) \right| \tag{20}$$

Physically, the left-hand side implies that we have more information (less uncertainty) in an entangled state than if the two states are treated separately, hence by treating the subsystems separately the correlations (entanglement) are being neglected. Also, equality in the left-hand side holds when both systems are independent for ρ_A, i.e., if the composite system is in a pure state, then S(ρ)=0, and from the right-hand side it follows that $S(\rho_A)=S(\rho_B)$ (Schmidt decomposition Eq. (13)).

As in the classical case, two important relations can be established (Wehrl, 1978), namely, the entropies of independent systems add up

$$S(\rho_A \otimes \rho_B) = S(\rho_A) + S(\rho_B) \tag{21}$$

Further, concavity reflects the fact that mixing states increases uncertainty, i.e.

$$S\left(\sum \lambda_i \rho_i\right) \geq \sum \lambda_i S(\rho_i) \tag{22}$$

According to the definition of the Shannon mutual information which relates only two observables, a quantum analog can be defined which measures the correlation between whole subsystems. The von Neumann mutual information between two subsystems ρ_A and ρ_B of a joint state ρ_{AB} is defined a

$$S(\rho_A : \rho_B) = S(\rho_A) + S(\rho_B) - S(\rho_{AB}) \tag{23}$$

As in the case of the Shannon mutual information this quantity can be interpreted as a distance between two quantum states, the correlated joint state (ρ_{AB}) and the uncorrelated one $\rho_A \otimes \rho_B$, which may be represented through a relative entropy

$$S(\rho_A : \rho_B) = S(\rho_{AB} \| \rho_A \otimes \rho_B) \tag{24}$$

Hence, the relative quantum entropy is an important quantity to classify and quantify quantum correlations (Wehrl, 1978; Vedral, 2002). This measure (Eq. 24) possesses important properties. It is invariant to unitary transformations (the distance between states can not be affected under a change in the basis)

$$S(\rho \| \sigma) = S(U\rho U^{+} \| U\sigma U^{+}) \tag{25}$$

Partial tracing over a part of the system produces a loss of information and hence the subsystems are more difficult to distinguish

$$S(Tr\rho \| Tr\sigma) \leq S(\rho \| \sigma) \tag{26}$$

Therefore, the relative entropy decreases under any combination of these two operations which means that quantum distinguishability never increases.
In order to determine the properties of any good measure of entanglement we have to establish that a bipartite state is "disentangled" if it is in a separable form

$$\rho_{AB} = \sum_i \lambda_i \rho_i^A \otimes \rho_i^B \tag{27}$$

These are the most general states that can be created by local operations and classical communication, Eqs (25) and (26), which contain no quantum correlations as entanglement can only be created through global operations (Wehrl, 1978; Vedral, 2002). Then in order to quantify entanglement is necessary to establish the following: (i) For a disentangled state (separable), the measure of entanglement should be zero, E(ρ)=0, (ii) under any local unitary transformations there is only a change of basis, which is completely reversible for the given entangled state, and then a change of basis should not change the amount of entanglement, i.e.,

$$E(\sigma) = E(U_A \otimes U_B \sigma U_A^{+} \otimes U_B^{+}) \tag{28}$$

Finally, local operations, classical communication and tracing of an ensemble σ which is transformed into subsystems σ_i with probabilities p_i, can not increase the expected entanglement. i.e.,

$$E(\sigma) \geq \sum_i p_i E(\sigma_i) \tag{29}$$

In summary we can conclude that in order to quantify quantum correlations between entangled subsystems, a good measure of quantum correlation has to be non-increasing under local operations (acting separately on A and B), and hence the only way the subsystems become entangled and gain information about each other is by interacting. We will return to this important conclusion in section 2.3.

2.3 Natural atomic probabilities in information theory

We have recently shown (Carrera et al., 2010) that there is an information-theoretic justification for performing Lowdin symmetric transformations (Löwdin, 1970) on the

atomic Hilbert space, to produce orthonormal atomic orbitals of maximal occupancy for the given wavefunction, which are derived in turn from atomic angular symmetry subblocks of the density matrix, localized on a particular atom and transforming to the angular symmetry of the atoms. This alternative information derivation (Carrera et al., 2010) was achieved by minimizing the entropy deficiency between the joint density ρ^{AB} (a reduced first density matrix of a composite fermionic system of the subsystems A and B) with respect to the atomic independent subsystems ρ^A and ρ^B, such that

$$\delta\left\{S\left(\rho^{AB}:\rho^A\otimes\rho^B\right)-\lambda(Tr(\rho^{AB})-1)\right\}=0 \tag{30}$$

according to the constraint

$$Tr(\rho^{AB})=1 \tag{31}$$

The advantages of these kind of atoms-in-molecules (AIM) approaches (Reed & Weinhold, 1983; Davidson, 1967)) are that the resulting natural atomic orbitals are *N*- and *v*-representables (Carrera et al., 2010), positively bounded, and rotationally invariant (Reed et al., 1985; Bruhn et al., 2006). An analogous information-theoretic approach was derived (Nalewajski, 2003) in relation with the Hirshfeld stockholder partitioning of the molecular electron density in Cartesian space (Hirshfeld, 1977).

2.4 Hilbert space partitioning in molecular fragments

We have proposed (Flores-Gallegos & Esquivel, 2008) that a molecule might be considered as a system formed by atomic subsystems, which could be studied through atomic or molecular fragments by means of natural atomic probabilities (Carrera et al., 2010). These probabilities are obtained by diagonalizing the atomic blocks (one center local transformation) of the molecular density matrix which transforms as angular symmetry representations of the isolated atoms, the resulting orthonormal orbitals are thus naturally optimal for the atom in the molecular binding environment. Then, the whole set of diagonalized atomic orbitals is symmetrically orthogonalized as to remove the interatomic overlap, while preserving the atom-like character of the orbitals as nearly as possible (Reed et al., 1985). Thus, the natural atomic probabilities are obtained by local unitary transformations and partial tracing of the molecular density matrix which should decrease the entanglement (Eqs. 26 and 29) by losing information between subsystems. The resulting density matrix is atomic-block diagonal and its spectral decomposition reduces to the atomic angular symmetry instead of the irreducible representation of the symmetry point group of the molecule, hence it can not be reduced to a convex sum of independent subsystems, and therefore its entanglement is not zero. It has been discussed that marginal density matrices with trace-class operators may have their own diagonal representations in terms of orthonormal and complete states in their respective subspaces which do not have marginal (subsystem) probabilities of the composite probability and as a result, the conditional entropies may be negative (Rajagopal et al., 2002); Cerf & Adami, 1997). In this study we have restricted ourselves to the study of a class of entropies (H-type) which possess marginal probabilities of molecular fragments. Thus, we may define atomic density operators through natural atomic probabilities in Cartesian space

$$\rho^A=\sum_{ilm}p_{ilm}(A)\left|\chi_{ilm}(A)\right|^2 \tag{32}$$

And then we may define molecular fragments in an analogous way

$$\rho^{M} = \sum_{A=1}^{M} \rho(A) \tag{33}$$

In Hilbert space we may define a measure of quantum correlations between molecular fragments for a bipartite system through natural atomic probabilities and their joint probability. As we mentioned before, in the study of a bipartite system decomposed through a Schmidt orthogonalization, there are no more than N states that might be entangled (Eqs. 15 and 16). In the natural atomic decomposition scheme we employ there are m states pertaining to molecular fragment A, i.e., $\{p_i(A);$ i= 1 to $m\}$ with n states corresponding to molecular fragment B: $\{ p_j(B)$; j= 1 to $n\}$, thus, we may define the joint entropy through global operations by correlating m x n states as providing that the following constraints are met:

$$\sum_i \sum_j P_{ij}(A,B) = \sum_i P_i(A) = \sum_j P_j(B) = \sum_i P_{ij}(A/B) = 1 \tag{34}$$

And the marginal probabilities are written as

$$P_{ij}(A \mid B) = \frac{P_{ij}(A,B)}{\sum_i P_{ij}(A,B)} \tag{35}$$

We are now in position of using definitions of section 2.1, related to the von Neumann entropies, taking into account that in our natural atomic scheme of probabilities, equality in Eq. (19) holds, and instead of referring to observables we deal with subsystems (molecular fragments), that is why von Neumann entropies are adequate for our study, though we keep the H-terminology to emphasize the orthogonal and commuting properties of the subspaces we are dealing with. It is easy to show that all relations concerning to $H(A)$, $H(B)$, $H(A,B)$, $H(A:B)$ and $H(A \mid B)$ are fulfilled with the definitions above (Eqs 1-11), along with some useful inequalities which follow immediately from definitions in Sec 2.1, i.e.,

$$\begin{aligned}
&H(A) \geq 0 \\
&H(A \mid B) \geq 0 \\
&H(A \mid B) \leq H(A) \\
&H(A,B) \leq H(A) + H(B) \\
&H(A:B) \geq 0 \\
&H(A:B) \equiv H(B:A) \\
&H(A,B) \equiv H(B,A) \\
&H(A,B) \geq H(A:B)
\end{aligned} \tag{36}$$

3. Chemical processes

Theoretic-information measures of the Shannon type have been employed to describe the course of the simplest hydrogen abstraction and the identity S_N2 exchange chemical reactions (Esquivel et al., 2009). For these elementary chemical processes, the transition state

is detected and the bond breaking/forming regions are revealed. A plausibility argument of the former is provided and verified numerically. It is shown that the information entropy profiles posses much more chemically meaningful structure than the profile of the total energy for these chemical reactions. Results support the concept of a continuum of transient of Zewail and Polanyi for the transition state rather than a single state, which is also in agreement with reaction force analyses. Furthermore, the information-theoretic description of the course of these elementary chemical reactions allowed a phenomenological description of their chemical behavior by use of Shannon entropic measures in position and momentum spaces. Interestingly, the analyses also revealed their synchronous/ asynchronous mechanistic behavior (Esquivel et al., 2010).

3.1 Phenomenological description of elementary chemical reactions

The prediction, from first principles, of the structure and energetics of molecules when exerting physical changes such as dissociations or chemical reactions, constitutes a major activity of theoretical/computational chemistry. Such an endeavour has not been an easy one though, involving several research areas which have provided solid grounds and fertile soil for theories and models that have pervaded over the years in ongoing research efforts that have been thoroughly discussed in the literature (Hoffman et al., 2003). We will briefly review here some of the ones that have brought up the need of characterizing chemical processes in terms of physical phenomena such as charge depletion/accumulation, bond breaking/forming, path reaction-following etc.

In an attempt to understand the stereochemical course of chemical reactions, calculations of potential energy surfaces have been carried out extensively at various levels of sophistication (Schlegel, 1988). Within the broad scope of these investigations, particular interest has been focused on extracting information about the stationary points of the energy surface. Considering the Born-Oppenheimer approximation, minima on the N-dimensional potential energy surface for the nuclei can be identified with the classical picture of equilibrium structures of molecules and saddle points can be related to transition states and reaction rates. Since the formulation of transition-state (TS) theory (Eyring, 1935; Wigner, 1939), a great effort has been devoted to developing models for characterizing the TS, which is assumed to govern the height of a chemical reaction barrier, so that any insights into the nature of the TS are likely to provide deeper understanding of the chemical reactivity. Computational quantum chemistry has sidestepped the inherent problems by managing rigorous mathematical definitions of "critical points" on a potential energy hypersurface, and hence assigned to equilibrium complexes or transition states. Within this approach, minima and saddle points have been fully characterized through the first and second derivatives of the energy (gradient and Hessian) over the nuclei positions. That is, if there is more than one minimum on a continuous energy surface, a family of paths can be obtained that connect one minimum to the other and if the highest energy point on each path is considered, the TS can be defined then as the lowest of these maxima along the reaction path, and a minimum for all displacements perpendicular to that path, i.e., a first-order saddle point. The eigenvector corresponding to the single negative eigenvalue of this critical point is the transition vector. It is so that the steepest-descent path from the saddle point to either of the two minima (reactants or products) follows this vector. Since the minima and the transition state are well defined points on the energy surface, it is possible to define a unique reaction path, though it would depend on the particular choice of the coordinate

system. This problem was solved by defining an intrinsic reaction path independently of the coordinate system by appealing to classical mechanics in which the motion equations are the simplest in mass-weighted Cartesian coordinates (Fukui, 1981). Then an intrinsic reaction coordinate (IRC) can be defined as the path traced by a classical particle moving with infinitesimal velocity from a saddle point down to the minima and the IRC is unique in virtue of the classical equations of motion which should be the same in any coordinate system. In mass-weighted coordinates the IRC and the steepest-descent path are the same. Several computational techniques which calculate energy gradients and Hessians have been developed to follow such reaction paths (González & Schlegel, 1990; Peng et al., 1996; Fan & Ziegler, 1992; Safi, 2001; Pople et al., 1978; González-García et al., 2006; Ishida, et al. 1977; Schmidt, et al. , 1985; Baskin et al., 1974).

Notwithstanding that critical points of the energy surface are useful mathematical features for analyzing the reaction-path, their chemical or physical meaning remains uncertain (Shaik, et al., 1994). Chemical concepts such as the reaction rate and the reaction barrier have been thoroughly studied and yet, the pursuit for understanding the TS structure represents a challenge of physical organic chemistry. The many efforts to achieve the latter have produced chemically useful descriptions of the TS such as the one provided by Hammond and Leffler (Hammond, 1955; Leffler, 1953). Hammond postulated that two points on a reaction profile that are of similar energy will also be of similar structure. This allowed predictions regarding the structure of the transition state to be made in highly exothermic and endothermic reactions. Leffler generalized the idea to the entire range of reaction exothermicities by considering the TS as a hybrid of reactants and products whose character is intermediate between these two extremes. These ideas remain as a very practical tool for analyzing chemical reactions now referred as to the Hammond-Leffler postulate which generally states that the properties of the TS are intermediate between reactant and product and are related to the position of the TS along the reaction coordinate.

With the advent of femtosecond time-resolved methods the aforementioned theories have turned out to be more relevant at the present time. Since the seminal studies of Zewail and co-workers (Zewail, 1988, 1990, 2000a, 2000b), femtochemistry techniques have been applied to chemical reactions ranging in complexity from bond-breaking in diatomic molecules to dynamics in larger organic and biological molecules, providing new insights into the understanding of fundamental chemical processes, on Zewail's words: "chemistry on the femtosecond time scale, can be defined as the field of chemical dynamics concerned with the very act of breaking or making a chemical bond. On this time scale the molecular dynamics are "frozen out", and thus one should be able to observe the complete evolution of the chemical event, starting from time zero, passing through transition states, and ultimately forming products". Although most femtochemistry studies deal with excited-state processes, ground-state processes have been studied as well. One of the most promising techniques, the anion photodetachment spectra (Bradforth, 1993), has made possible the direct observation of transition states. In order to explain the experimental results of the femto-techniques it would be necessary to complement the existing chemical reactivity theories with electronic density descriptors of the events taking place in the vicinity of the transition-state region, where the chemical bonds are actually being formed or destroyed.

In connection with the above, there are a number of studies in the literature which have employed a variety of descriptors either to study the TS structure or to follow the course of the chemical reaction path. For instance, Shi and Boyd performed a systematic analysis of

model S_N2 reactions in order to study the TS charge distribution in connection with the Hammond-Leffler postulate (Shi & Boyd, 1991). Bader et al developed a theory of reactivity based solely on the properties of the charge density by employing the properties of the Laplacian of the density so as to align the local charge concentrations with regions of charge depletion of the reactants by mixing in the lowest energy excited state of the combined system to produce a relaxed charge distribution corresponding to the transition density (Bader & MacDougall, 1985). By studying the time evolution of a bimolecular exchange reaction Balakrishnan & Sathyamurthy (1989) showed that information-theoretic entropies in dual or phase space rised to a maximum in a dynamical study. Following the course of two elementary S_N2 reactions, Ho et al showed that theoretic-information measures were able to reveal geometrical changes of the density which were not present in the energy profile, although the transition states were not apparent from the study (Hô et al., 2000). In an attempt to build a density-based theory of chemical reactivity, Knoerr and Eberhart (2001), reported correlations between features of the quantum mechanically determined charge density and the energy-based measures of Shaik and collaborators to describe the charge transfer, stability, and charge localization accompanying an S_N2 reaction (Shaik et al., 1992). Moreover, Tachibana (2001) was able to visualize the formation of a chemical bond of selected model reactions by using the kinetic energy density to identify the intrinsic shape of the reactants, the TS and the reaction products along the course of the IRC, hence realizing Coulson's conjecture (1991) in that the physical meaning of the probability density might be related with the energy density. The reaction force of a system's potential energy along the reaction coordinate has been employed to characterize changes in the structural and/or electronic properties in chemical reactions (Toro-Labbé, et al., 2009; Toro-Labbé et al., 2007; Murray et al., 2009; Jaque et al., 2009) . The Kullback–Leibler information deficiency has been evaluated along molecular internal rotational or vibrational coordinates and along the intrinsic reaction coordinate for several S_N2 reactions (Borgoo et al., 2009).

Notwithstanding that there has been a great interest in the last twenty years in applying Information Theory (IT) measures to the electronic structure of atoms and molecules (Gadre, 2003; Koga & Morita, 1983; Ghosh et al., 1984; Angulo & Dehesa, 1992; Antolín et al., 1993; Angulo, 1994; Massen & Panos, 1998; Ramirez et al., 1998; Nalewajski & Parr, 2001; Nagy, 2003; Romera & Dehesa, 2004; Karafiloglou & Panos, 2004; Sen, 2005; Parr et al. , 2005; Guevara et al., 2005; Shi & Kais, 2005; Chatzisavvas et al., 2005; Sen & Katriel, 2006; Nagy, 2006; Ayers, 2006; Martyusheva & Seleznev, 2006; Liu, 2007), it has not been clearly assessed whether theoretic-information measures are good descriptors for characterizing chemical reaction parameters, i.e., the stationary points of the IRC path (the TS and the equilibrium geometries of the complex species) and the bond breaking/forming regions. The purpose of the study was to perform a phenomenological description of two selected elementary chemical reactions by following their IRC paths with the purpose of analyzing the behaviour of the densities in position and momentum spaces, at the vicinity of the TS, and also at the regions of bond forming/breaking that are not visible in the energy profile, by use of the Shannon entropies in conjugated spaces. In order to witness the density changes exerted by the molecular structures and link them with the theoretic-information quantities during the chemical processes, we will employ several charge density descriptors such as the Molecular Electrostatic Potential (MEP) and some reactivity parameters of Density Functional Theory (DFT), the hardness and the softness. The chemical probes under study are the simplest hydrogen abstraction reaction $H^{\bullet} + H_2 \longrightarrow H_2 + H^{\bullet}$ and the identity S_N2 reaction $H_a^- + CH_4 \longrightarrow CH_4 + H_b^-$.

The central quantities under study are the Shannon entropies in position and momentum spaces (Shannon, 1948), which are analogous to Eq. (1) for the case of the continuous variable distributions, $\rho(\mathbf{r})$ and $\gamma(\mathbf{p})$:

$$S_r = -\int \rho(\mathbf{r}) \ln \rho(\mathbf{r}) d^3\mathbf{r} \tag{37}$$

$$S_p = -\int \gamma(\mathbf{p}) \ln \gamma(\mathbf{p}) d^3\mathbf{p} \tag{38}$$

where $\rho(\mathbf{r})$ and $\gamma(\mathbf{p})$ denote the molecular electron densities in the position and momentum spaces, each normalized to unity. The Shannon entropy in position space S_r behaves as a measure of delocalization or lack of structure of the electronic density in the position space and hence S_r is maximal when knowledge of $\rho(\mathbf{r})$ is minimal and becomes delocalized. The Shannon entropy in momentum space S_p is largest for systems with electrons of higher speed (delocalized $\gamma(\mathbf{p})$) and is smaller for relaxed systems where kinetic energy is low. Entropy in momentum space S_p is closely related to S_r by the uncertainty relation of Bialynicki-Birula and Mycielski (1975), which shows that the entropy sum $S_T=S_r+S_p$, is a balanced measure and cannot decrease arbitrarily. For one-electron atomic systems it may be interpreted as that localization of the electron's position results in an increase of the kinetic energy and a delocalization of the momentum density, and conversely.

In connection with the behaviour of the Shannon entropies above discussed, we expect a simple theoretic-information description of the TS in terms of localized/delocalized distributions. Considering that there is no variational principle for any quantum-mechanical property other than the energy, deriving a direct relation between the TS and the Shannon entropies as functionals of the electron densities seems not practical and surely beyond the scope of the present work. Instead, we present a plausible physical argument to link both quantities: on mathematical grounds the TS represents a first-order saddle point connecting two minima in a topological sense, and physically it represents a maximum in the "potential energy" surface (PES) within the space of all possible nuclear configurations corresponding to the energetically easiest passage from reactants to products constrained to the Born-Oppenheimer approximation. In this sense, TS structure posses (locally) the highest potential energy among all possible chemical structures in that path at the expense of a minimum kinetic energy. Since the transition state theory (Eyring, 1935; Wigner, 1938) is essentially based on the assumption that atomic nuclei behave according to classic mechanics, the presumption for the TS being represented by a chemical structure with a minimum kinetic energy, which corresponds with a highly localized momentum density (locally), seems justified. Simultaneously, the TS will require a highly delocalized density in position space for the uncertainty principle to be satisfied. In this sense the Shannon entropies, as logarithmic descriptors of the electron density distributions in the combined phase space (normalized to unity), would correspond to extrema on the entropy profile at the vicinity of the TS, provided that the densities are adequately represented in the chemical space.

The MEP represents the molecular potential energy of a proton at a particular location near a molecule (Politzer & Truhlar, 1981), say at nucleus A. Then the electrostatic potential , V_A , is defined as

$$V_A = \left(\frac{\partial E^{molecule}}{\partial Z_A} \right)_{N, Z_{B \neq A}} = \sum_{B \neq A} \frac{Z_B}{|R_B - R_A|} - \int \frac{\rho(\mathbf{r}) dr}{|\mathbf{r} - R_A|'} \tag{39}$$

where $\rho(\mathbf{r})$ is the molecular electron density and Z_A is the nuclear charge of atom A, located at R_A. Generally speaking, negative electrostatic potential corresponds to an attraction of the proton by the concentrated electron density in the molecules from lone pairs, pi-bonds, etc… (coloured in shades of red in standard contour diagrams). Positive electrostatic potential corresponds to repulsion of the proton by the atomic nuclei in regions where low electron density exists and the nuclear charge is incompletely shielded (coloured in shades of blue in standard contour diagrams).

We have also evaluated some reactivity parameters that may be useful to analyze the chemical reactivity of the processes. Parr and Pearson (1983), proposed a quantitative definition of hardness (η) within conceptual DFT:

$$\eta = \frac{1}{2S} = \frac{1}{2}\left(\frac{\partial \mu}{\partial N}\right)_{v(r)} \tag{40}$$

where $\mu = \left(\frac{\partial E}{\partial N}\right)_{v(r)}$ is the electronic chemical potential of an N electron system in the presence of an external potential ν(**r**), E is the total energy and "S" is called the softness within the context of DFT. Using finite difference approximation, Eq. (39) would be

$$\eta = \frac{1}{2S} \approx \frac{\left(E_{N+1} - 2E_N + E_{N-1}\right)}{2} = \frac{(I - A)}{2} \tag{41}$$

where E_N, E_{N-1} and E_{N+1} are the energies of the neutral, cationic and anionic systems; and I and A, are the ionization potential (IP) and electron affinity (EA), respectively. Applying Koopmans' theorem (Koopmans, 1933; Janak, 1978), Eq. (4) can be written as:

$$\eta = \frac{1}{2S} \approx \frac{\varepsilon_{LUMO} - \varepsilon_{HOMO}}{2} \tag{42}$$

where ε denotes the frontier molecular orbital energies. In general terms, hardness and softness are good descriptors of chemical reactivity, the former measures the global stability of the molecule (larger values of η corresponds to less reactive molecules), whereas the S index quantifies the polarizability of the molecule (Ghanty & Ghosh, 1993; Roy et al., 1994; Hati, & Datta, 1994; Simon-Manso & Fuenteaelba, 1998), thus soft molecules are more polarizable and possess predisposition to acquire additional electronic charge (Chattaraj et al., 2006). The chemical hardness "η" is a central quantity for use in the study of reactivity and stability, through the hard and soft acids and bases principle (Pearson, 1963; 1973; 1997). However, in many cases, the experimental electron affinity is negative rather than positive, an such systems pose a fundamental problem; the anion is unstable with respect to electron loss and cannot be described by a standard DFT ground-state total energy calculation. To circumvent this limitation, Tozer and De Proft have introduced an approximate method to compute this quantity, requiring only the calculation of the neutral and cationic systems which does not explicitly involve the electron affinity (Tozer & De Proft, 2005):

$$\eta = \frac{\varepsilon_{LUMO} - \varepsilon_{HOMO}}{2} + \varepsilon_{HOMO} + I \tag{43}$$

where *I* is obtained from total electronic energy calculations on the *N-1* and *N* electron systems at the neutral geometry $I = E_{N-1} - E_N$ and all energy quantities have to be calculated by continuum approximations such as the local exchange-correlation functionals (GGA) to avoid integer discontinuities. Nevertheless, it has been observed that expression (43) does still work reasonably well with hybrids, such as B3LYP (Tozer & De Proft, 2005). The authors have shown that this approximate method (Eq. 43) provided reasonable estimates for the electron affinities of systems possessing metastable anions, such as the case of CH_4 with large negative experimental electron affinity (-7.8 eV). We have employed Tozer and De Proft approach for computing the hardness of the S_N2 ionic complex in order to test this approximation in a process departing from the ground-state requirement such as the IRP (Intrinsic Reaction Process) of a chemical reaction (De Proft, 2008).
The electronic structure calculations performed in the present study were carried out with the Gaussian 03 suite of programs (Frisch et al., 2004). Reported TS geometrical parameters for the abstraction (Johnson, 1994), and the S_N2 exchange reactions were employed (Shi & Boyd, 1989). Internal reaction coordinate (IRC) calculations (González & Schlegel, 1989) were performed at the MP2 (UMP2 for the abstraction reaction) level of theory with at least 35 points for each one of the reaction directions (forward/reverse) of the IRC path. Then, a high level of theory and a well balanced basis set (diffuse and polarized orbitals) were chosen for determining all the properties for the chemical structures corresponding to the IRC path according to the strategy followed in Esquivel et al., 2009. The hardness and softness chemical parameters were calculated by use of Eqs. (42) and (43) and the standard hybrid B3LYP (UB3LYP for the abstraction reaction) functional (Tozer & De Proft, 2005). Molecular frequencies corresponding to the normal modes of vibration depend on the roots of the eigenvalues of the Hessian (its matrix elements are associated with force constants) at the nuclei positions of the stationary points. We have found illustrative to calculate these values for the normal mode associated with the TS (possessing one imaginary frequency or negative force constant) which were determined analytically for all points of the IRC path at the MP2 (UMP2 for the abstraction reaction) level of theory (Frisch, 2004). The molecular information entropies in position and momentum spaces for the IRC path were obtained by employing software developed in our laboratory along with 3D numerical integration routines (Pérez-Jordá & San-Fabián, 1993; Pérez-Jordá et al., 1994), and the DGRID suite of programs (Kohout, 2007). The bond breaking/forming regions along with electrophilic/nucleophilic atomic regions were calculated through the MEP by use of MOLDEN (Schaftenaar & Noordik, 2000). Atomic units are employed throughout the Chapter unless otherwise is stated.

3.1.1 Radical abstraction reaction

The reaction $H^{\bullet} + H_2 \longrightarrow H_2 + H^{\bullet}$ is the simplest radical abstraction reaction involving a free radical (atomic hydrogen in this case) as a reactive intermediate. This kind of reaction involves at least two steps (S_N1 like): in the first step a new radical is created by homolysis and in the second one the new radical recombines with another radical species. Such homolytic bond cleavage occurs when the bond involved is not polar and there is no electrophile or nucleophile at hand to promote heterolytic patterns. When the bond is made, the product has a lower energy than the reactants and it follows that breaking the bond requires energy. Evidence has been presented (Esquivel et al., 2010) which shows that the two step mechanism observed for this type of reaction is completely characterized by an asynchronous behaviour but yet "concerted".

Our calculations for this reaction were performed at two different levels, the IRC was obtained at the UMP2/6-311G level and all properties at the IRC path were obtained at the QCISD(T)/6-311++G** level of theory. As a result of the IRC, 72 points evenly distributed between the forward and reverse directions of the reaction were obtained. A relative tolerance of $1x10^{-5}$ was set for the numerical integrations (Pérez-Jordá & San-Fabián, 1993; Pérez-Jordá et al., 1994).

In Fig. 1, the energy profile for the process is depicted against the intrinsic reaction coordinate (R_X) which shows the symmetric behavior of the IRC path. Also, in Fig. 1 we have depicted the entropy sum, which shows the exact opposite behavior as that of the energy, i.e., the TS represents a chemical structure with a localized density in the combined space of position and momentum (dual or phase space), which corresponds to a more delocalized position density with the lowest kinetic energy (more localized momentum density) among all the structures at the vicinity of the IRC path (see below). In this way the saddle point might be characterized by IT in the entropy hyper-surface.

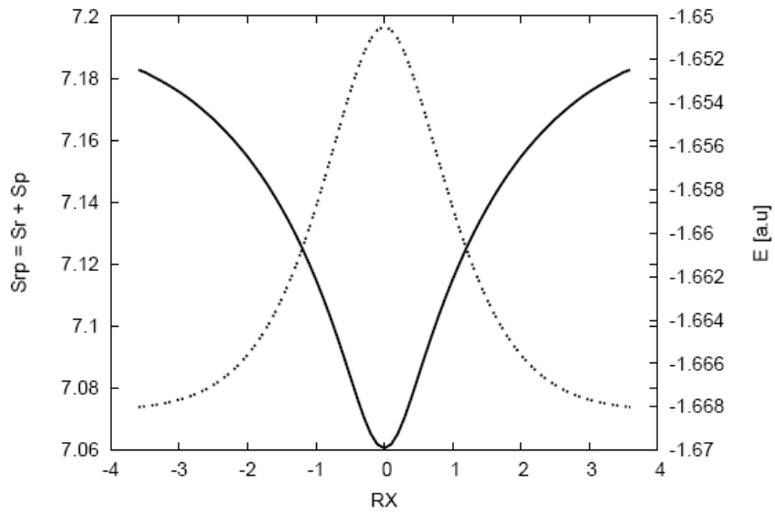

Fig. 1. Total energy values (dashed line) in a.u. and the entropy sum (solid line) for the IRC path of $H_a^{\bullet} + H_2 \longrightarrow H_2 + H_b^{\bullet}$

The Shannon entropies in position and momentum spaces for the abstraction reaction are depicted in Fig. 2 in order to characterize their critical points at the IRC path by use of several density descriptors discussed below. At first glance, we may note from Fig. 2 that the position entropy possesses a local maximum at the TS and two minima at its vicinity, whereas the momentum entropy possesses a minimum at the TS with two maxima at its vicinity, hence we observe that both quantities behave in opposite ways, i.e., the Shannon entropy in position space shows larger values toward the reactant/product complex ($H_a^{\bullet}\cdots H\text{-}H_b$ or $H_a\text{-}H\cdots H_b^{\bullet}$) and tends to decrease toward the TS region. In contrast, the momentum entropy increases as the intermediate radical ($H_a^{\bullet}$) approaches the molecule, reaching maxima at the vicinity of the TS. This behaviour is interpreted as follows: the position entropy values are smaller at the vicinity of the TS region as compared with the ones at the reactive complex region (towards reactants and products) since the densities of the chemical structures are globally more localized at the TS region (see Fig. 1 in connection

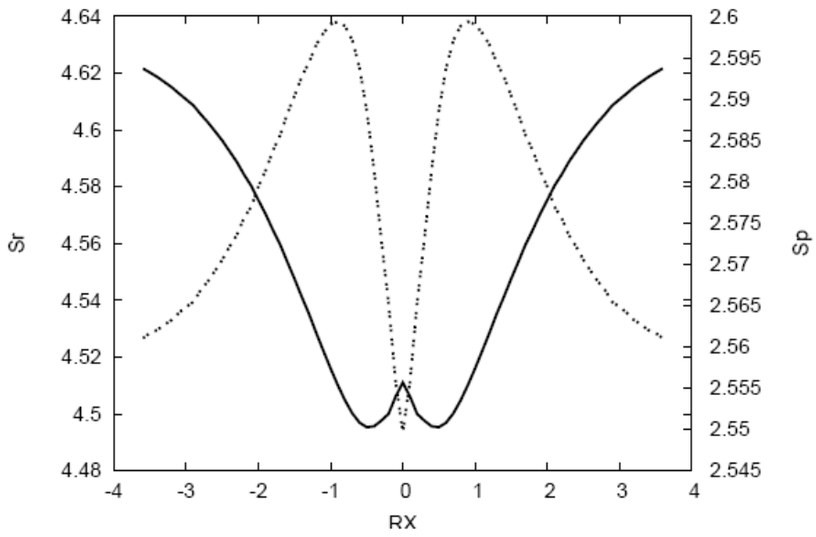

Fig. 2. Shannon entropies in position (solid line) and momentum (dashed line) spaces for the IRC path of $H_a^{\bullet} + H_2 \longrightarrow H_2 + H_b^{\bullet}$

with the entropy sum), which is the zone where the important chemical changes take place. On the perspective of the momentum entropy, we may note that it is minimal at the TS which is linked to a more localized momentum density possessing the lowest kinetic energy value (maximum at the potential energy surface). At the reactive complex regions, momentum entropy values are larger than at the TS and therefore the corresponding kinetic energies are larger too, hence reproducing the typical potential energy surface shown in Fig. 1. In Fig. 3, the bond distances (in Angstroms) between the entering/leaving hydrogen radicals and the central hydrogen atom are depicted. This clearly shows that in the vicinity of the TS a bond breaking/forming chemical situation is occurring since the R_{in} is elongating at the right side of the TS and the R_{out} is stretching at the left side of the TS. It is worth

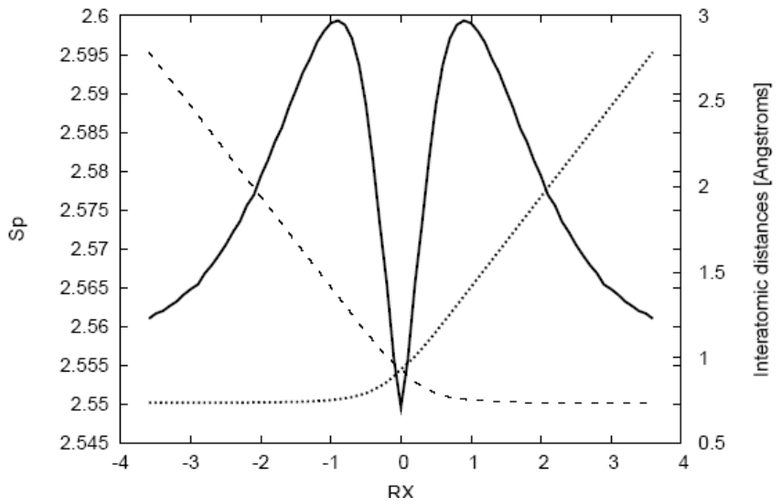

Fig. 3. Shannon entropy in momentum space (solid line) and the bond distances $R(H_0\text{-}H_{in})$ (dashed line for the entering hydrogen) and $R(H_0\text{-}H_{out})$ (dotted line for the leaving hydrogen) in Angstroms for the IRC path of $H_a^{\bullet} + H_2 \longrightarrow H_2 + H_b^{\bullet}$

noting that the chemical process does not happen in a concerted manner, i.e., the homolytic bond breaking occurs first and then the molecule stabilizes by forming the TS structure which is clearly observed in the Fig. 3. As the incoming radical approaches the molecule the bond breaks, at the same location where the position entropy is minimum and the momentum entropy is maximum, then the TS is reached and the new molecule is formed afterwards. This is in agreement with the discussion above with regard to the two step mechanism characterizing this reaction.

The non-polar bond pattern characteristics of homolytic bond-breaking kind of reactions has been studied through the dipole moment of the molecules at the IRC path (Esquivel et al., 2009). This is indeed observed in Fig. 4, where these values along with the ones of the momentum entropy are depicted for comparison purposes. At the TS the dipole moment is zero, and the same is observed as the process tends to the reactants/products in the reaction path, reflecting the non-polar behavior of the molecule in these regions. However, it is also interesting to observe from this property, how the molecular densities get distorted, reaching maximal values at the vicinity of the TS, where the position entropies are minimal, i.e., at the bond breaking/forming regions the complex exerts its largest distortion, molecular geometry gets rigid where the position density is more localized. Once more, we may observed from Fig. 4 that the energy reservoirs for the bond cleavage occur earlier (or later depending on the direction of the reaction) at the IRC path as observed from the maxima of the momentum entropies. We will refer to these chemical regions as to bond cleavage energy reservoirs (BCER) in what follows.

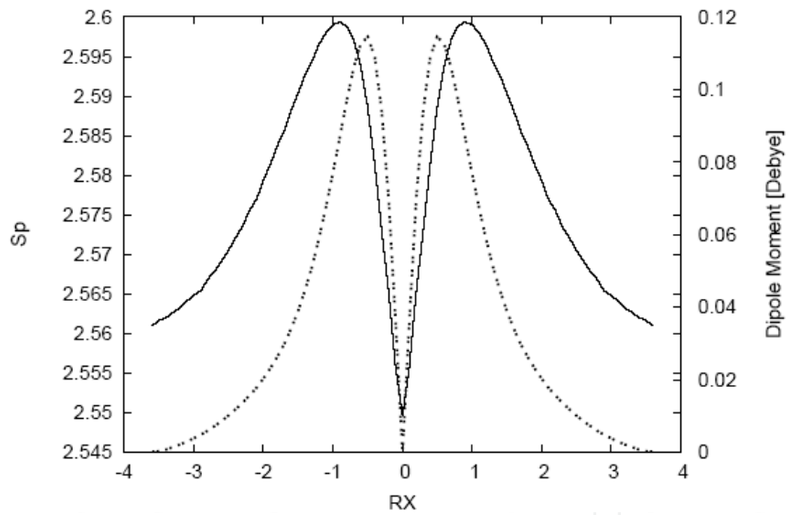

Fig. 4. Shannon entropy in momentum space (solid line) and the dipole moment values in Debye (dashed line) for the IRC path of $H_a^{\bullet} + H_2 \longrightarrow H_2 + H_b^{\bullet}$.

In Fig. 5 the eigenvalues of the Hessian for the normal mode associated with the TS along the path of the reaction are depicted along with the momentum entropy values for comparison purposes. These Hessian values represent the transition vector "frequencies" which show maxima at the vicinity of the TS and a minimal value at the TS. Several features are worth mentioning, the TS corresponds indeed to a saddle point, maxima of the Hessian correspond to high kinetic energy values (largest "frequencies" for the energy cleavage reservoirs) since they fit with maximal values in the momentum entropy profile, and the Hessian is minimal at the TS, where the kinetic energy is the lowest (minimal molecular

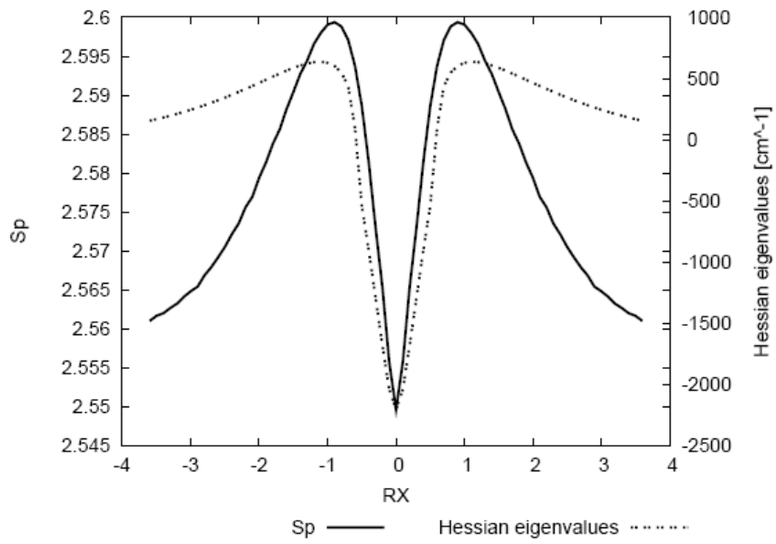

Fig. 5. Shannon entropy in momentum space (solid line) and the eigenvalues of the Hessian (dashed line) for the IRC path of $H_a^{\bullet} + H_2 \longrightarrow H_2 + H_b^{\bullet}$. It should be noted that negative values actually correspond with imaginary numbers (roots of negative force constants) so that the negative sign only represents a flag.

frequency) and it corresponds to a minimal momentum-entropy value. Furthermore, the transition state of a reaction is commonly identified by the presence of a negative force constant for one normal vibrational mode corresponding with an imaginary frequency. The work of Zewail and Polanyi in transition state spectroscopy has led to the concept of a reaction having a continuum of transient, a transition region rather than a single transition state (Zewail, 1988; 1990; 2000a; 2000b; Polanyi & Zewail, 1995). It is worth mentioning that the results of the present study show indeed the existence of such a region between the BCER, before and after the TS. This is in agreement with reaction force, *F(R)*, studies (Toro-Labbé, et al., 2009; Toro-Labbé et al., 2007; Murray et al., 2009; Jaque et al., 2009) where the reaction force constant, *κ(R)*, also reflects this continuum, showing it to be bounded by the minimum and the maximum of *F(R)*, at which *κ(R) = 0*.

The chemical reactivity behavior of the reaction has also been analyzed through density descriptors such as the hardness and softness (Esquivel et al., 2009). From a DFT conceptual point of view, chemical structures with maximal hardness (minimal softness) possess low polarizability and hence are less propense to acquire additional charge (less reactive). These structures are found at the BCER regions, they are maximally distorted, with highly localized position densities (Esquivel et al., 2009).

3.1.2 Hydrogenic identity S_N2 exchange reaction

Continuing with the study of elementary chemical reactions it is of interest to analyze a typical nucleophilic substitution (S_N2) reaction since its chemical process involves only one step in contrast with the two-step S_N1 reaction. In the anionic form, the S_N2 mechanism can be depicted as $Y^- + RX \rightarrow RY + X^-$, which is characterized by being kinetically of second order (first order in each of the reactants; the nucleophile $Y^-$and the substrate RX, where X^- is the nucleofuge or leaving atom). For identity S_N2 reactions X=Y. It was postulated that the observed second order kinetics is the result of passage through the well-known Walden

inversion transition state where the nucleophile displaces the nucleofuge (leaving group) from the backside in a single concerted reaction step. Evidence has been presented (Esquivel et al., 2010) which shows that the one step mechanism observed for this type of reaction is indeed characterized by its synchronous and concerted behaviour.

The $H_a^- + CH_4 \longrightarrow CH_4 + H_b^-$ represents the typical identity S_N2 reaction and we proceed with the calculations as follows: since diffuse functions are important to adequately represent anionic species (Shi & Boyd, 1991), we have performed calculations for the IRC at the MP2/6-311++G** level of theory, which generated 93 points evenly distributed between the forward and reverse directions of the IRC. Then, all entropies and geometrical parameters at the IRC path were calculated at the QCISD(T)/6-311++G** level of theory which has been reported to be adequate for this kind of reactions (Glukhovtsev et al., 1995). A relative tolerance of $1x10^{-5}$ was set for the numerical integrations (Pérez-Jordá & San-Fabián, 1993; Pérez-Jordá et al., 1994).

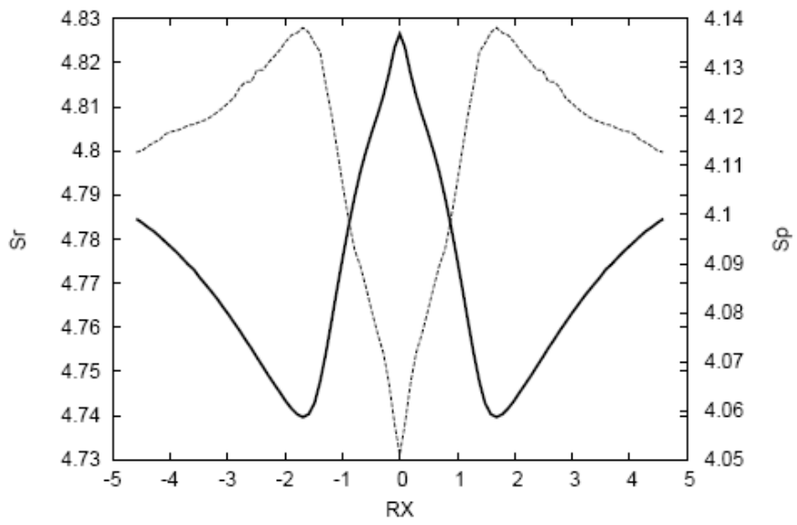

Fig. 6. Shannon entropies in position (solid line) and momentum (dashed line) spaces for the IRC path of the S_N2 reaction at the QCISD(T)/6-311++G** level.

A comparison between the entropy sum (see Fig. 7) and the energy shows that both quantities behave in an opposite manner, although the entropy sum shows much more structure at the vicinity of the TS region as compared to the energy profile (Esquivel et al., 2009). The nature of the richer structure observed for the entropy sum (as compared with the energy) was revealed through the position and momentum entropies depicted in Fig. 6 which show a TS structure characterized by a delocalized position density and a localized momentum density, i.e., corresponding with a structurally relaxed structure with low kinetic energy. In contrast, as compared with the TS; the reactive complex toward reactants/products show more localized position densities with less localized momentum densities, i.e., the chemical structures at these regions are structurally distorted and posses more kinetic energy as compared with the TS. At the vicinity of the TS, at around $|R_X| \approx 1.7$, critical points for both entropies are observed, minima/maxima for the position/momentum entropies, respectively. Thus, ionic complex at these regions characterize position densities which are highly localized and with highly delocalized momentum densities and high kinetic energies. At first glance, it seems likely that these

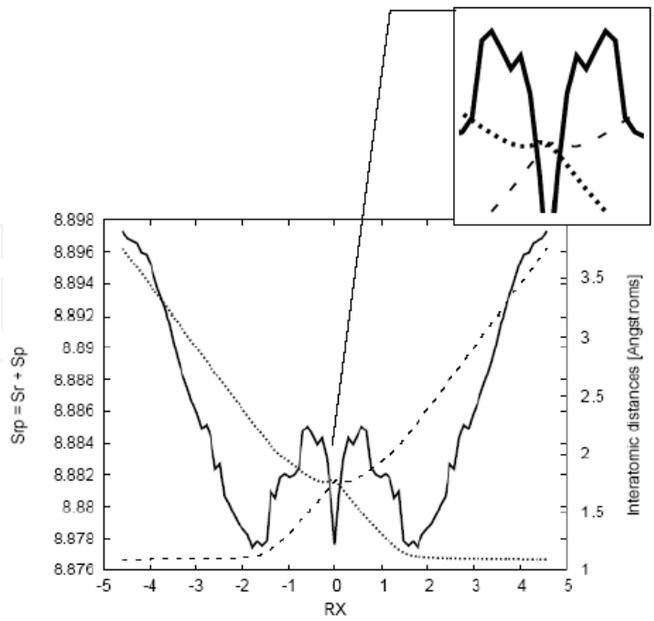

Fig. 7. Shannon entropy in momentum space (solid line) and the bond distance R_a (dotted line), corresponding to the H_a-C distance, and R_b (dashed line) corresponding to the (C-H_b) distance for the IRC path of the S_N2 reaction. In the side frame: detail of the minima observed for the bond distances at $R_X \approx -0.3$. Distances in Angstroms.

regions correspond with BCER where bond breaking may start occurring. Two more features that are worth noting is that both entropies show inflection points at $|R_X| \approx 1.0$ and maxima at $|R_X| \approx 0.5$, regions where the entropy sum shows more defined structure (see Fig. 7), change of curvature and maxima, respectively (Esquivel et al., 2009). We will come back later to these observations in connection with other properties.

In order to support our observations above we find instructive to plot the distances between the incoming hydrogen (H_a) and the leaving hydrogen (H_b) in Fig. 7. Distances show the stretching/elongating features associated with the bond forming/breaking situation that we have anticipated before. In contrast with the previous analyzed abstraction reaction, the S_N2 reaction occurs in a concerted manner, i.e., the bond breaking/forming starts taking place at the same time, in a gradual and more complicated manner as we explain below. An interesting feature which might be observed from Fig. 7 is that whereas the elongation of the carbon-nucleofuge (C-H_b) bond (R_b) changes its curvature significantly at $R_X \approx -1.7$ (forward direction of the reaction) the stretching of the nucleophile-carbon (H_a-C) bond (R_a) does it in a smooth way, posing the argument that bond breaking is occurring first, due to the repulsive forces that the ionic molecule exerts as the nucleophile approaches which provokes the breaking of the carbon-nucleofuge to happen as the molecule starts liberating its kinetic energy (decrease of the momentum entropy). In this sense is that the reaction occurs in a concerted manner, i.e., the bond-breaking/dissipating-energy processes occurring simultaneously. At the near vicinity of the TS, around $R_X \approx -0.3$, we observe small changes for both interatomic distances revealed through minima in the amplified picture, where it is apparent that repulsive forces occur at the TS. Moreover, the analysis of the internal angle between H_a-C-H along with the Shannon entropy in position space for comparison purposes. Thus, the internal angle shows clearly that the molecule starts

exerting the so called "inversion of configuration" at around $R_X \approx -1.7$, where the nucleophile starts displacing the nucleofuge from the backside in a single concerted reaction step. This starts occurring at the BCER regions (see above).
Fig. 8 shows the repulsive effect we mentioned before in connection with the interatomic distances (Fig. 7) by noting that the leaving atom Hb is gaining nucleophilic power (negative MEP). The TS state which is not depicted shows a half and half electrophilic/nucleophilic character among the atoms, where the charge is evenly distributed throughout the molecule.

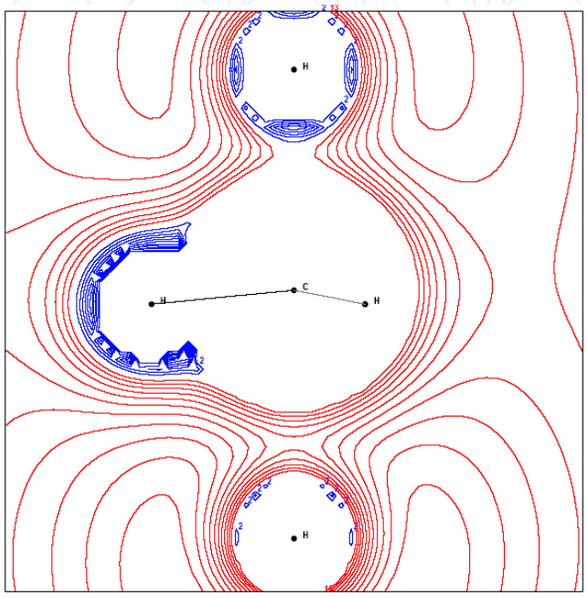

Fig. 8. The MEP contour lines in the plane of H_a-C-H_b (H_a stands for the nucleophilic atom and H_b is the nucleofuge, on bottom and top, respectively) showing positive MEP (nucleophilic regions) and negative MEP (electrophilic regions) at $R_X \approx -0.3$ for the S_N2 reaction.

The S_N2 reaction is an excellent probe to test the polar bond pattern characteristic of heterolytic bond-breaking (with residual ionic attraction because of the ionic nature of the products) which should be reflected through the dipole moment of the molecules at the IRC path (note that the origin of the coordinate system is placed at the molecules's center of nuclear charge). This is indeed observed in Fig. 9, where these values along with the ones of the momentum entropy are depicted for comparison purposes. At the TS the dipole moment is zero showing the non polar character of the TS structure with both nuclephile/nucleofuge atoms repelling each other evenly through its carbon bonding. At this point the momentum/position entropies are minimal/maximal reflecting the low kinetic energy feature of the chemically relaxed TS structure. As the reactive complex approach the reactants/products regions the dipole moment increases monotonically reflecting the polar bonding character of the ionic complex with a significant change of curvature at the TS vicinity at around $|R_X| \approx 1.0$ (a change of curvature was already noted for all entropies at the same region). In going from reactants to products it is evident that the inversion of the dipole moment values reflects clearly the inversion of configuration of the molecule (this reaction starts with a tetrahedral sp^3 carbon in the methyl molecule and ends with a tetrahedral sp3 in the product), which is an inherent feature of S_N2 reactions.

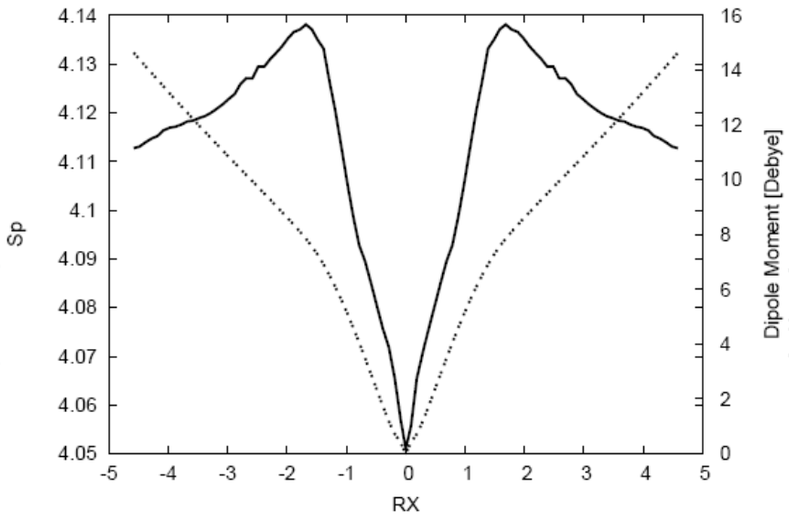

Fig. 9. Shannon entropy in position space (solid line) and the total dipole moment (dotted line) for the IRC path of the S_N2 reaction. Dipole moment in Debye.

It is interesting to note that as in the case of the hydrogenic abstraction reaction, the eigenvalues of the Hessian (Esquivel et al., 2009) for the normal mode associated with the TS along the IRC path show maxima at the BCER and reach their minimal value at the TS. This again validates the concept of a continuum of transient of Zewail and Polanyi, i.e., a transition region rather than a single transition state (see above).

3.2 Reaction mechanisms

A reaction mechanism represents a sequence of elementary steps by which overall chemical change occurs, describing in detail what it takes place at each stage of a chemical transformation, such as the bonds that are being formed or broken, and in what order. The chemical course of a reaction also accounts for the order in which molecules react, either by single- or multi-step conversions, and provides information about the structure of the transition state, reactive complexes, kinetics, catalysis, and stereochemistry. In this section we present a theoretical ab initio study which presents evidence obtained from Shannon theoretic-information concepts in position and momentum spaces that allow a conceptual description of the course of two elementary chemical reactions, revealing all the expected physical transformations predicted for synchronous (one-step) and non-synchronous (two-step) reaction mechanisms.

Dewar (1984) has employed intuitive arguments along with numerical evidence to put forward the notion of "synchronicity being normally prohibited for multibond processes", which is in contrast with the widely accepted Woodward-Hoffman rules (Woodward & Hoffmann, 1969) that establish that multibond "allowed" reactions must be synchronous, i.e., all the bond-forming and bond-breaking processes taking place simultaneously. Furthermore, it has been asserted (Bernasconi, 1992) that a principle for non-perfect synchronization might be derived from the realization that the majority of elementary reactions involve more than one concurrent molecular process such as bond formation/cleavage, delocalization/localization of charge, etc. and that often these processes have made unequal progress at the transition state. For instance, one bond mechanisms are predominant in elementary processes of organic chemistry and most

chemists believe these take place in a synchronous manner. Recently, the simplest prototypical hydrogen exchange reaction (Chandra, 1996) and a variety of other radical exchange reactions have been examined (Chandra, 1999) by use of *ab initio* methods to conclude that despite the fact that these reactions are chemically classified as being concerted (taking place in a single kinetic step) their bond-cleavaging processes are slightly more advanced than the bond-forming ones, proceeding by a two-stages mechanism (Dewar, 1984), and therefore they show asynchronous features.

There has been an increasing interest in the recent years to analyse the electronic structure of atoms and molecules by applying Information Theory (IT) (Gadre, 2003; Koga & Morita, 1983; Ghosh et al., 1984; Angulo & Dehesa, 1992; Antolín et al., 1993; Angulo, 1994; Massen & Panos, 1998; Ramirez et al., 1998; Nalewajski & Parr, 2001; Nagy, 2003; Romera & Dehesa, 2004; Karafiloglou & Panos, 2004; Sen, 2005; Parr et al. , 2005; Guevara et al., 2005; Shi & Kais, 2005; Chatzisavvas et al., 2005; Sen & Katriel, 2006; Nagy, 2006; Ayers, 2006; Martyusheva & Seleznev, 2006; Liu, 2007 These studies have shown that information-theoretic measures are capable of providing simple pictorial chemical descriptions of atoms and molecules and the processes they exert through the localized/delocalized behaviour of the electron densities in position and momentum spaces. In a recent study (Esquivel et al., 2009), we have provided with evidence which supports the utility of the theoretic-information measures in position and momentum spaces to detect the transition state and the stationary points of elementary chemical reactions so as to reveal the bond breaking/forming regions of the simplest hydrogen abstraction and the identity S_N2 exchange chemical processes, thus providing evidence of the concept of a reaction having a continuum of transient of Zewail and Polanyi and also in agreement with reaction force analysis (see above).

The purpose of the present study is to follow the IRC path of the simplest hydrogen abstraction reaction $H_a^{\bullet} + H_2 \longrightarrow H_2 + H_b^{\bullet}$ and the exchange identity S_N2 reaction $H_a^{-} + CH_4 \longrightarrow CH_4 + H_b^{-}$, with the purpose of performing a phenomenological description of two selected elementary chemical reactions with different mechanistic courses by use of Shannon theoretic-information measures in both conjugated spaces, position and momentum.

Abstraction reactions proceed by homolysis and can be characterized by a mechanism being kinetically of first order (S_N1 like). These kind of reactions involve a two-step mechanism, which initiates with the formation of a new radical created by homolysis and continues with the recombination of the new radical with another radical species. Such homolytic bond cleavage occurs when the bond involved is non polar and there is no electrophile or nucleophile at hand to promote heterolytic patterns. When the bond is made, the product has a lower energy than the reactants and it follows that breaking the bond requires energy. In contrast, the hydride-exchange reactions proceed by a S_N2 mechanism which is characterised by being kinetically of second order (first order in each of the reactants: the nucleophile and the nucleofuge atoms). It has been postulated that the observed second order kinetics is the result of passage through the well-known Walden inversion transition state where the nucleophile displaces the nucleofuge (leaving group) from the backside in a single concerted reaction step.

The reaction $H_a^{\bullet} + H_2 \longrightarrow H_2 + H_b^{\bullet}$ is the simplest radical abstraction reaction involving a free radical, $H_a^{\bullet}$ or $H_b^{\bullet}$, as a reactive intermediate (reaction A) whereas the $H_a^{-} + CH_4 \longrightarrow CH_4 + H_b^{-}$ is a typical S_N2 identity exchange reaction (reaction B), where H_a^{-} represents the incoming nucleophile and H_b^{-} stands for the leaving nucleofuge. The electronic structure calculations performed in this study were carried out with the Gaussian

03 suite of programs (Frisch et al., 2004). The reported TS geometrical parameters for the abstraction (Johnson, 1994), and the S_N2 exchange reactions (Shi & Boyd, 1989) were employed. Calculations for the structures of the internal reaction path were performed by use of the IRC method at the MP2/6-311++G** (UMP2//6-311G for the abstraction reaction) level of theory. As a result of the latter, 72/93 points (chemical structures) evenly distributed on the forward and reverse directions of the IRC paths were obtained for the A/B reactions, respectively. Finally, a higher level of theory (QCISD(T)) and a properly balanced basis set (6-311++G**) were chosen for both reactions to calculate the Shannon entropies of all chemical structures at the IRC paths. The molecular Shannon information entropies were obtained by employing software developed in our laboratory along with 3D numerical integration routines (Pérez-Jordá & San-Fabián, 1993; Pérez-Jordá et al., 1994), and the DGRID suite of programs (Kohout, 2007).

For reaction A (Fig. 2), both entropies possess richer structure at the vicinity of the TS as compared with the energy profile (which only shows one maximum at this point). By close inspection of Fig. 2, we note that the position entropy possesses a local maximum at the TS and two minima at its vicinity, whereas the momentum entropy decreases abruptly so as to reach a global minimum at the TS with two maxima at its vicinity.

The chemical picture proceeds in this way: as the intermediate radical ($H_a^{\bullet}$) approaches the molecule at the TS region, the molecular density exerts important changes so as to undergo the homolysis. This represents a physical situation where the density in position space gets localized in preparation for the bond rupture, which in turn results in a local increase of the kinetic energy. This provides explanation for well the known fact that bond breaking requires energy. Next, the bond is formed and as a consequence, the TS structure shows lower kinetic energy than the reactant/product complex ($H_a^{\bullet}\cdots H\text{-}H_b$ or $H_a\text{-}H\cdots H_b^{\bullet}$). Interestingly, from an information-theoretic perspective all of the above can be analogously described as observed in Fig. 2: as the radical intermediate approaches the TS region, the position entropies turn minimal when the position densities become localized and the corresponding momentum densities get delocalized (higher kinetic energies). Then at the TS, when the chemical structure relaxes, the position/momentum density gets delocalized/localized where the position/momentum entropy shows a local maximum/ minimum. The process occurs in two steps in the way the reaction dictates, and this also might be observed from the theoretic-information context by closely examining the entropies behaviour at the proximity of the TS. That is, the bond breaking process requires energy which should in turn be dissipated by relaxing the structure at the TS, and we note from Fig. 2 that this is indeed the case in that maxima for the momentum entropy are located before minima of the position entropy (depending on the direction of the process), i.e., reactive complexes gain the necessary energy for bond cleavage at BCER (bond cleavage energy regions and then get localized as we described above. Next, the homolysis provokes energy/density relaxation of the molecules toward the TS which is also observed from the Shannon entropies as explained before.

For reaction B (Fig. 6), again both Shannon entropies show richer structure as compared to the total energy profile (which only possesses one maximum at the TS). By examining Fig. 6 we note that the position entropy profile features a maximum at the TS along with two minima at its vicinity, whereas the profile of the momentum entropy shows a global minimum at the TS with two maxima at its vicinity. It seems likely that these particular regions correspond with BCER where bond breaking is supposed to occur. It is interesting to note that for both entropies the BCER are located at the same IRC coordinate, in contrast

with the two-stages mechanism of reaction A, and this may be indicative of the single step mechanism that characterizes the S_N2 process, which highlights the localized/delocalized combination of the position/momentum densities at this particular position of the IRP. At this point, it is interesting to associate the one step mechanism of this reaction to the chemical events that take place. While the nucleophile approaches the molecule the nucleofuge leaves it at unison, i.e., bond forming and bond breaking must occur in a concerted and synchronous manner. Both of these actions increase the energy of the combination: bond breaking requires energy (momentum density becomes delocalized and its corresponding entropy increases, and so its kinetic energy) as does overcoming the repulsion between the incoming ionic-complex (nucleophile) into close contact with the carbon's bonding shell (position density becomes localized and its corresponding entropy decreases). As the reaction process goes forward, the energy increases until a significant bonding begins to occur between the nucleophile and the molecule (increasing the position entropy and delocalizing its density). This releases enough energy to balance the energy required to break the carbon-nucleofuge bond (low kinetic energy structure with a highly localized momentum density). Then the transition state is reached. It is worth mentioning that the abrupt changes apparently observed for the Shannon entropies in both reactions (Figs. 2 and 6) are largely due to the significant changes exerted by the densities at the vicinity of the TS within the BCER (Esquivel et al., 2009).

4. Nanostructured materials

On the perspective of much larger molecules, Shannon Information Theory (IT) has been employed to analyze the growing behavior of nanostructures (Esquivel, 2009b). Shannon entropies in position and momentum spaces require costly and time-consuming computations as the size of the molecules increases in contrast with information entropies in Hilbert space, which are shown to be highly advantageous for analyzing large molecules. Thus, ab initio electronic structure calculations at the Hartree-Fock level of theory were performed to characterize the initial steps towards growing nanostructured molecules of Polyamidoamine (PAMAM) dendrimers, starting from the monomers, dimers, trimers, tetramers up to generations G0 (with 84 atoms), G1 (228 atoms), G2 (516 atoms), and G3 (1092 atoms). Shannon and Kullback entropies in Hilbert space were employed to provide theoretic-information evidence of the validity of the dense-core model of PAMAM precursors and dendrimers G0 through G3. Furthermore, marginal H-type von Neumann informational entropies (Flores-Gallegos & Esquivel, 2008) have been employed (Esquivel, 2010b) to provide evidence of the validity of the dense-core model of dendrimers.

4.1 Information-theoretical analysis of selected PAMAM dendrimers

Since their introduction in 1985 by Tomalia (Tomalia et al., 1985) dendrimers have attracted much attention because of their fascinating structure and unique properties (Newkome et al., 1996; Fréchet & Tomalia, 2001) Dendrimers are globular, size monodisperse macromolecules in which all bonds emerge radially from a central focal point or core with a regular branching pattern and with units that repeat and contribute to a branch point. They are defined by three components: a central core, an internal dendritic structure (the branches), and an exterrnal surface with functional surface groups. Not all regularly branched molecules are dendrimers because properties of the dendritic state (Fréchet &

Tomalia, 2001), such as core encapsulation (Hecht & Fréchet, 2001). Several applications for dendrimers have been proposed in the literature (Tomalia et al., 1990), with potential applications in biology as mimetic systems of enzymes or redox proteins (Liu & Breslow, 2003), in medicine for drug delivery, gene therapy, and biochemical sensors (Zeng & Zimmerman, 1997)., in optoelectronics for transduction of signals or light-harvesting devices (Vögtle, 2000) and in nanoscience as building units in self-assembled systems or functionalized with groups for molecular recognition and signaling (Fréchet, 2002). Among these, Poly(amido)amine or PAMAM dendrimers are among the most studied families of dendrimers. These organic dendrimers contain tertiary amines as branching points, i.e., the respective branching multiplicity is 2. The core multiplicity varies; the original PAMAM dendrimers were synthesized from an amine core and thus had a 3-fold multiplicity (Newkome et al., 1996; Liu & Breslow, 2003) whereas recently, ethylenediamine-core PAMAMs became more common and these have a 4-fold multiplicity (Jockush et al., 1999) where the typical end-groups are primary amines.

A number of review articles on dendrimers have been reported (Ballauff, 2001; Newkome, 2001). Most of the work was motivated by a dendrimer-model of a hollow core and hence by a dense shell. This model became popular since the work of de Gennes and Hervet (1983) in which they presented the first theoretical treatment of dendrimers where they obtained a density profile with a global minimum at the center and a monotonic density increasing towards the periphery of the dendrimer. On the other hand, Lescanec and Muthukumar (1990) used a kinetic growth algorithm to find, in contrast with precvious studies (de Gennes & Hervet, 1983), density profiles that decreased monotonically towards the edge of the molecule. They were the first to show that a dendritic structure made up from flexible bonds should exhibit its maximum density at the center of the molecule becoming in the so-called dense-core model.

A great deal of progress in the understanding of the conformations of dendrimers has been achieved through computer simulations at various levels of description, from the microscopic (atomistic) to the oversimplified ones with different methodologies: Monte-Carlo (MC), molecular dynamics (MD), and Brownian dynamics (BD) (Allen & Tildesley, 1987). Recently, Maitli et al (2004), performed a systematic series of fully atomistic MC-MD simulations on PAMAM-ethylenediamine (PAMAM-EDA) cored dendrimers from G0 through G11, to characterize the structure and properties of these molecules. On the electronic structure (ES) side, only a few Hartree-Fock (HF) and density functional theory (DFT) studies have addressed to study some aspects of low order generation dendrimers (Tarazona-Vasquez & Balbuena, 2004a; 2004b). However, ab initio studies of the ES type addressing the structural properties of PAMAM dendrimers of higher generations are very scarce. The issue is not a simple one since these molecules possess an enormous number of energetically permissible conformations and a large number of atoms (EDA-PAMAM dendrimers grow from 84 atoms for G0 up to 294852 atoms for G11) which are beyond the present capabilities for the ES packages and present computers.

In recent imvestigations (Esquivel et al., 2009b; 2010b) we have shown that despite the limitations of quantum chemistry methods, it is possible to apply information.theory and chemical concepts to elucidate some of the structural features of dendrimers. The focus was on supporting the validity of the core-dense model for dendrimers from a theoretic information point of view. Besides, the growing behavior of PAMAM precursors and some low generations of its dendrimers was revealed by employing selected properties of soft physics matter along with chemical reactivity parameters of dendrimers.

It is known that flexible-chain dendrimers, although being chemically regular structures, do not assume regular shapes. To quantitatively evaluate the deviation from spherical symmetry, we calculated the shape of the precursors and dendrimers through the principal moments of inertia I_x, I_y and I_z which are calculated through the eigenvalues of the shape tensor **G** describing the mass distribution:

$$G_{pq} = (1/M)[\sum_{i}^{N} m_i(\mathbf{r}_{pi} - \mathbf{R}_p)(\mathbf{r}_{qi} - \mathbf{R}_q) \tag{44}$$

where $p,q = x,y,z$, and $\boldsymbol{r}_{pi}$ is the position of the ith atom relative to the R_p components of the center of mass of the molecule, M is the mass of the molecule and m_i is the mass of the atom. The sum of three eigenvalues (I_x, I_y and I_z) is an invariant of the shape tensor **G**, giving $\left\langle R_g^2 \right\rangle$, which is the mean-square radius of gyration that provides a quantitative characterization of the dendrimer size. The ratio of these three principal moments is a measure of *eccentricity* (minor-major axes ratio) of the shape ellipsoid of the dendrimers and hence the shape of the dendrimer can be assessed from the values of the ratio of the three principal moments of inertia of the molecules I_z/I_y and I_z/I_x. Rudnick and Gaspari (1986) introduced a better definition of *asphericity* frequently used in the literature as

$$\delta = 1 - 3\frac{\left\langle I_2 \right\rangle}{\left\langle I_1^2 \right\rangle} \tag{45}$$

where I_i are the respective invariants of the gyration tensor and are given by

$$I_1 = I_x + I_y + I_z \tag{46}$$

and

$$I_2 = I_x I_y + I_x I_z + I_y I_z \tag{47}$$

Technical details concerning the electronic structure calculations for the present study have been amply discussed (Esquivel et al., 2009b; 2010b). So that, the values of the three principal moments of inertia (Eqs. 46 and 47) were tabulated (see Esquivel, et al, 2010) along with the radius of gyration and the asphericity factor. Figure 10 shows the radius of gyration (Eq. 44), for the different G0-precursors and the G0 dendrimer. From the Figure (and Table 2 in Ref. 96) we may assess the size of the dendrimers through the radius of gyration. As expected, R_g values show a constant increasing trend in going from the monomers up to the G0-dendrimer.

On the side of the chemical reactivity of the precursors and dendrimers we have also evaluated some parameters that might be useful to analyze the chemical properties. In the context of conceptual DFT we have defined several properties in subsection 2.1 (Eqs. (40) to (43)), in particular hardness (η) and softness (S), which are good descriptors of chemical reactivity, the former measures the global stability of the molecule (larger values of η means less reactive molecules), whereas the S index quantifies the polarizability of the molecule (Ghanty & Ghosh, 1993; Roy et al., 1994), thus soft molecules are more polarizable and possess predisposition to acquire additional electronic charge (Chattaraj et al., 2006). It has been noted in Ref. Esquivel et al, 2010 that hardness values show a decreasing tendency as

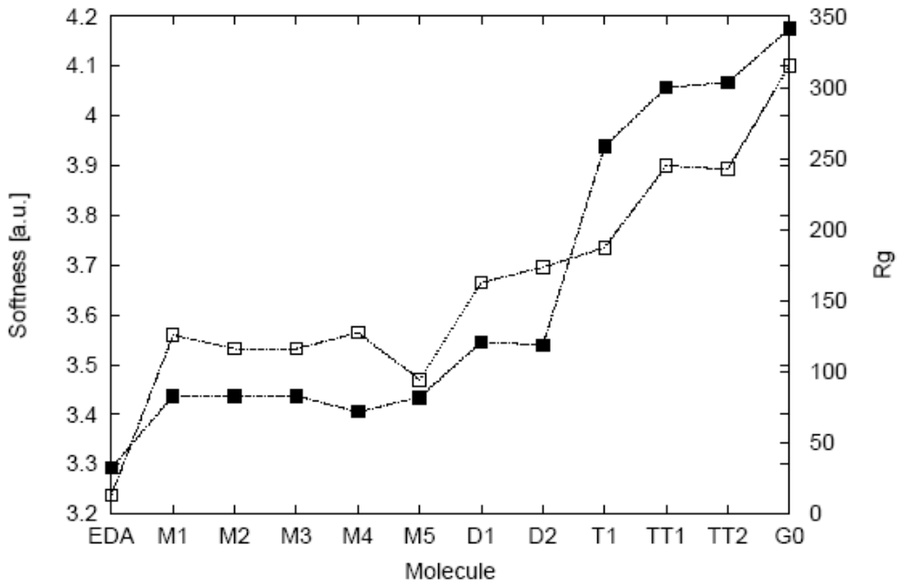

Fig. 10. The softness "S" (empty boxes) and the radius of gyration R_g (solid boxes) values for the G0-precursors and G0-PAMAM generation.

the molecules are sizely bigger, which means that as the size of the precursor increases toward G0 the polarizability of the molecules increases, i.e., their corresponding densities tend to be more delocalized. Further, it is known that less compact molecules are more polarizable, with low hardness values and hence more reactive, and this is indeed the case when comparing the softness values with the size of the molecules through the radius of gyration R_g in Figure 10.

4.2 Information-theoretical analysis of selected PAMAM dendrimers

Next, we examine the Shannon information entropies in real space, Eqs (37) and (38). In Figure 11 the entropy sum (S_r+S_p) and the energy are depicted for the PAMAM G0-precursors and dendrimer G0. It is apparent from Fig. 11 that the total entropy follows the opposite behavior as the energy, i.e., as the size of the molecules increases so does the entropy sum. It is also interesting to note that the total entropy distinguishes the different polymeric structures in that isoelectronic systems possess the same entropy value and so does the energy.

4.3 Information-theoretical entropies in hilbert space

We have recently shown (Carrera, E. M. et al., 2010) that there is an information-theoretic justification for performing Löwdin symmetric transformations (Löwdin, 1970; Reed & Weinhold, 1983; Davidson, 1967). on the atomic Hilbert space, to produce orthonormal atomic orbitals of maximal occupancy for the given wavefunction, which are derived in turn from atomic angular symmetry subblocks of the density matrix, localized on a particular atom and transforming to the angular symmetry of the atoms. The advantages of these kind of atoms-in-molecules (AIM) approaches (Reed et al., 1985; Bruhn et al., 2006) are that the resulting natural atomic orbitals are *N*-representables, positively bounded, and rotationally invariant. We have recently shown (Flores-Gallegos & Esquivel, 2008) that the corresponding

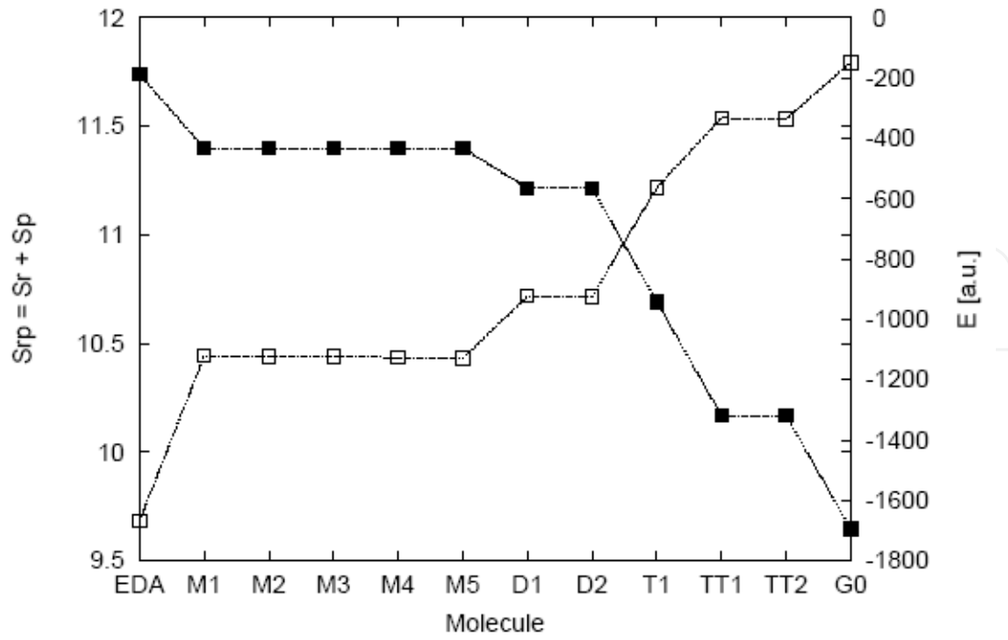

Fig. 11. Shannon entropy sum form Eqs. 1 and 2 (empty boxes) and the Energies in a.u. (solid boxes) for the PAMAM polymeric precursors at the HF/3-21G* level.

"natural atomic probabilities" (NAP) (Carrera, E. M. et al., 2010) are useful to define von Neumann information entropies in Hilbert space which might be able to measure entanglement in the context of Quantum Information Theory (Wehrl, 1978; Vedral, 2002).
The uncertainty of a probability distribution p_i(A) is measured through the Shannon entropy (Shannon, 1948) in Hilbert space Eq. (1). The relative entropy between two probability distributions p_i(A) and p_i(B) is defined through the Kullback-Liebler entropy (Kullback & Leibler, 1951) in Eq. (2) where the p_i(A) (and p_i(B)) in Eqs. (1) and (2) can be determined by use of natural atomic probabilities (Carrera et al., 2010; Flores-Gallegos & Esquivel, 2008). While Eq. (13) represents a distance from a reference probability which is not symmetrized.
Finally, we investigated the information entropies in Hilbert space in connection with the growing behavior of PAMAM dendrimers. It is important to mention that whereas Shannon entropies in real space represent costly and time consuming calculations, Hilbert space entropies do not pose additional computational efforts as to the theoretic-information analyses concerns, of course the obtaining of the wave functions and the NAP values represent a challenge for electronic structure calculations and the present computation capabilities available to us. Thus, we have performed the necessary calculations for analyzing additional structures, the trimer conformations T2 trhough T4, along with G1 through G3 dendrimers (G1 with 228 atoms, G2 with 516 atoms, and G3 with 1092 atoms). In Figure 12 we have depicted the Shannon entropy *H(A)* for all the PAMAM G0-precursors along with the G0 through G3 dendrimers. This measure allows to determine the global information content of the systems and consequently we may observe from Fig. 12 that *H(A)* shows an increasing behavior as the size of the precursors and dendrimers increases. This again supports the above discussed dense-core model of dendrimers as bigger molecules show more uncertainty in Hilbert space, which corresponds to less compact densities in real space and hence to more delocalized electronic distributions.

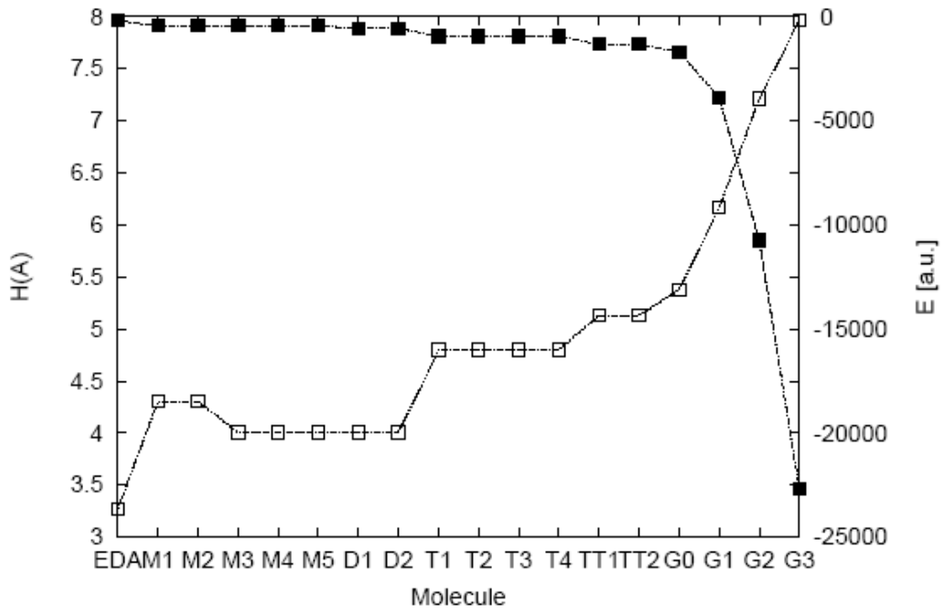

Fig. 12. Shannon entropy in Hilbert space, *H(A)* from Eq. (1) (empty boxes), and the total Energy values in a.u. (solid boxes) for the G0-precursors and generations G0 through G3.

Furthermore, in Figures 13 and 14 we have plotted the *H(A)* values along with the Kullback-Leibler relative entropy in Hilbert space, Eqs. (1) and (2), respectively. The *H(A | B)* measure represents a distance measure from a reference probability distribution, which in this case we have set for the EDA molecule (which is embedded in all the structures). We may observe from the Fig. 14 that as the molecules depart from EDA the Hilbert information distance increases in a monotonically fashion which reflects the core-dense growing behavior

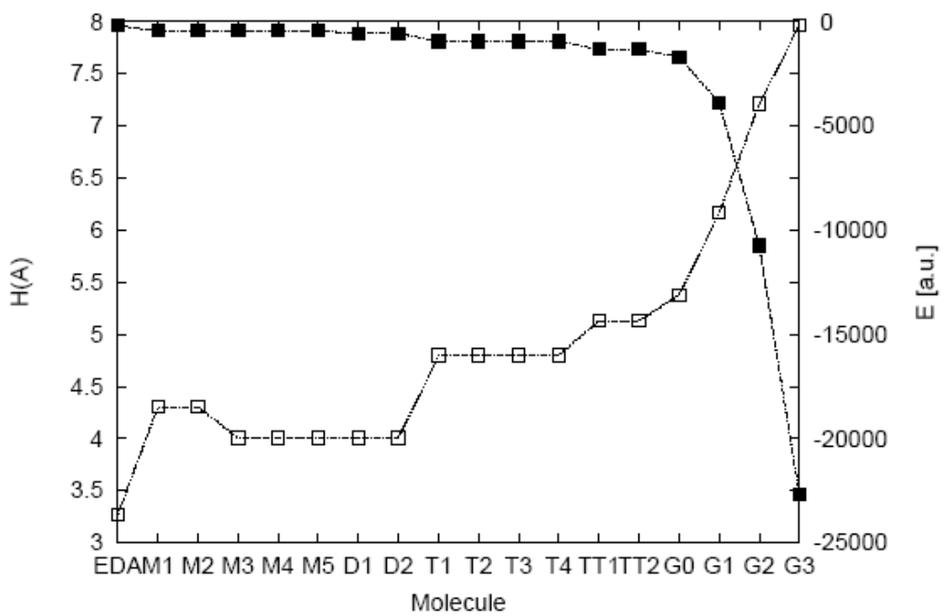

Fig. 13. Shannon entropy in Hilbert space, *H(A)* from Eq. (1) (empty boxes), and the total Energy values in a.u. (solid boxes) for the G0-precursors and generations G0 through G3.

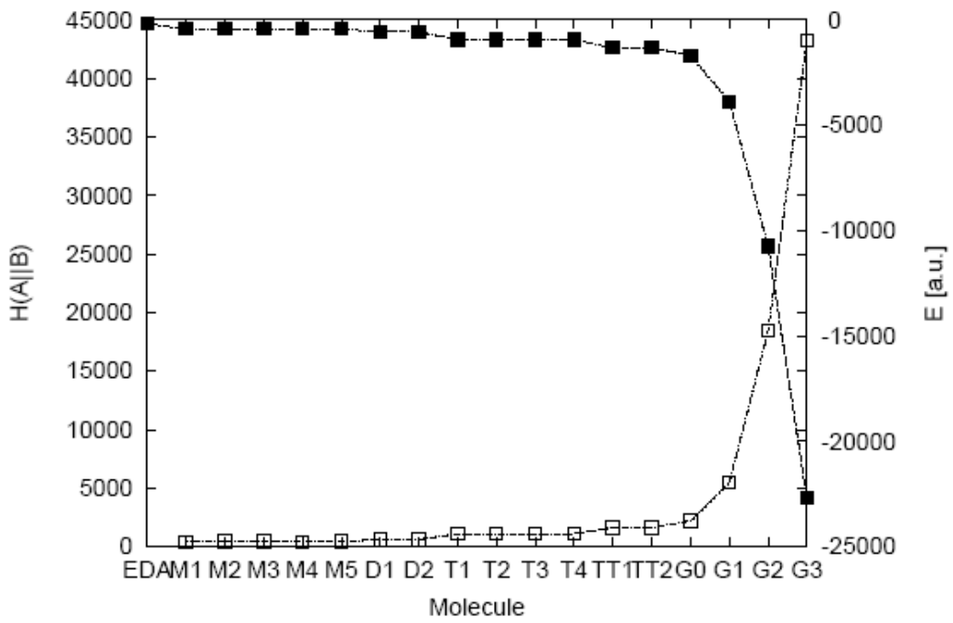

Fig. 14. Kullback-Leibler entropy in Hilbert space, *H(A | B)* from Eq. (2) (empty boxes), and the total Energy values in a.u. (solid boxes) for the G0-precursors and generations G0 through G3.

of dendrimers by simply measuring the information distance between EDA and the increasingly bigger molecules. Assuming that dendrimers follow a hollow-core model of growth and hence a dense shell model, the *H(A | B)* trend would have been just the opposite.

Figures 13 and 14 show the ability of these quantum measures to reveal and corroborate two simple facts already discussed in the literature (Löwdin, 1970): (i) the validity of the core-dense model witnessed by the mutual von Neumann entropy of the marginal type, as the *H(A | B)* Hilbert distance increases monotonically in going from the precursors to higher generation dendrimers, and (ii) the global information content of the systems, *H(A),* which increases monotonically as one would expect from a thermodynamic point of view (entropy). A particular feature that may be noted from Figure 13 is the capacity of *H(A)* of measuring the atomic and electronic content of the systems, regardless of its conformational structure, which is characteristic of the energy. The relevancy of these results might be assessed by considering that the equivalent information in real space implied the calculation of position and momentum space entropies of the Shannon type which, taking into account the size of the systems (1023 atoms for G3 dendrimer), represents indeed a formidable task to compute, even by taking into consideration that the integration quadratures were guided by promolecular grids (Esquivel et al., 2009b). Ongoing research is being undertaken in our laboratories to extend the study to higher generation PAMAM dendrimers mainly on the side of the Hilbert space framework.

5. Concluding remarks

We have shown throughout this Chapter that phenomenological description of chemical phenomena is readily acesible through Information Theory concepts of the Shannon type.

Moreover, it is worth mentioning that other recently published results have extended these ideas to more intrincated processes involving a three-center insertion reaction (Esquivel et al., 2010c), and in a more comprehensive manner in elementary chemical reactions and conformeric analysis through the local information measure of Fisher (López Rosa et al, 2010; Esquivel et al., 2011) and also by use of statistical complexity measures and planes (Esquivel et al., 2010d; 2011b). Furthermore, we have extended the scope of the analyses to quantum information concepts to measure the entanglement for the dissociation of diatomic molecules (Esquivel et al., 2011c).

Throughout these studies in several areas of chemistry and also in nanostructured systems, we believe that information science may conform a new scientific language to explain essential aspects of chemical phenomena (and presumably biological too). These new aspects are not accessible through any other standard methodology in quantum chemistry, allowing to reveal intrincated mechanisms in which chemical phenomena occur. This envisions a new area of research that looks very promising as a standalone and robust science. The purpose of our research is to provide fertile soil to build this nascent scientific area of chemical inquiry through information-theoretical concepts which we have named Quantum Information Chemistry.

The following aspects are to be distinguished from the studies:

i. We have assessed the utility for the theoretic-information measures of the Shannon type to characterize elementary chemical reactions. Through these chemical probes we were capable to observe the basic chemical phenomena of the bond breaking/forming showing that the Shannon measures are highly sensitive in detecting these chemical events not revealed by the energy profile. Furthermore, the transition state of a reaction is commonly identified by the presence of a negative force constant for one normal vibrational mode corresponding with an imaginary frequency. However the work of Zewail and Polanyi in transition state spectroscopy has led to the concept of a reaction having a continuum of transient, a transition region rather than a single transition state (Zewail, 1988; 1990; 2000a; 2000b; Polanyi & Zewail, 1995). It is worth mentioning that the results of the present study show indeed the existence of such a region between the BCER, before and after the TS. This is in agreement with reaction force, *F(R),* studies (Toro-Labbé, et al., 2009; Toro-Labbé et al., 2007; Murray et al., 2009; Jaque et al., 2009) where the reaction force constant, $\kappa(R)$, also reflects this continuum, showing it to be bounded by the minimum and the maximum of *F(R)*, at which $\kappa(R) = 0$.
ii. We have also shown (Esquivel et al., 2010) that theoretic-information measures of the Shannon type posses the capability of revealing the hidden structure of the chemical reactions through phenomenological concepts (Esquivel et al., 2009) which permit to unveil the asynchronous/synchronous mechanistic behavior which characterize reactions A and B, respectively. Furthermore, it is worth mentioning that the chemical phenomena treated here are largely invisible for most of the standard density descriptors, and certainly not accessible from the energy profile. We believe that this kind of studies may serve to provide with more specific information as to nourish chemical reactivity theories which pursue a full conceptual prediction of the TS structure from basic chemical principles (Shaik et al., 1992). On the other hand, it is our contention that these observations might be amenable of experimental verification through photodetachment techniques in the femtosecond time scale (Zewail, 1988, 1990, 2000a, 2000b).

iii. Throughout this investigation we have employed selected density descriptors which show numerical evidence which supports the dense-core model of dendrimers Besides, from a information-theoretical perspective, it was shown that Shannon entropies defined in real space as well as in Hilbert space are capable of revealing the dense core growing behavior of dendrimers, by showing that bigger molecules possess more delocalized electronic distributions in such a way to span their molecular distributions as the molecular size increases.

6. Acknowledgments

We wish to thank José María Pérez-Jordá and Miroslav Kohout for kindly providing with their numerical codes. We acknowledge financial support through Mexican grants from CONACyT, PIFI, PROMEP-SEP and Spanish grants MICINN projects FIS2011-24540, FQM-4643 and P06-FQM-2445 of Junta de Andalucía. J.A., J.C.A., R.O.E. belong to the Andalusian researchs groups FQM-020 and J.S.D. to FQM-0207. R.O.E. wishes to acknowledge financial support from the Ministerio de Educación of Spain through grant SAB2009-0120 and to Prof. Marcelo Galván for his valuable support. Allocation of supercomputing time from Laboratorio de Supercómputo y Visualización at UAM, Sección de Supercomputacion at CSIRC Universidad de Granada, and Departamento de Supercómputo at DGSCA-UNAM is gratefully acknowledged.

7. References

Allen, M. P. & Tildesley, D. J. (1987). Computer Simulation of Liquids, Clarendon, Oxford, 1987;

Angulo, J. C. & Dehesa, J. S. (1992). J. Chem. Phys. 1992, 97, 6485-6495

Angulo, J. C. (1994). Phys. Rev. A 1994, 50, 311-313

Antolín, J.; Zarzo, A. & Angulo, J. C. (1993). Phys. Rev. A 1993, 48, 4149-4155.

Araki, H. & E. H. Lieb (1970). Commun. Math. Phys. 1970, 18, 160.

Ayers, W. (2006). Theor. Chem. Acc. 2006, 115, 253-256

Bader, R.F.W. & MacDougall P.J. (1985). J. Am. Chem. Soc. 1985, 107, 6788-6795

Balakrishnan N. & Sathyamurthy, N. (1989). Chem. Phys. Lett. 1989, 164, 267-269

Ballauff, M. (2001). Dendrimers III: Design, Dimension, Function:, Top. Curr. Chem. 212, (2001) 177–194

Baskin, C.P.; Bender, C.F.; Bauschlicher, C.W. Jr.; & Schaefer III, H.F. J. Am. Chem. Soc. 1974, 96, 2709-2713

Bell, J (1987).*Speakable and Unspeakable in Quantum Mechanics* 1987 (Cambridge University, Cambridge).

Bernasconi, C.F. (1992). Acc. Chem. Res. 25 (1992) 9.

Bialynicky-Birula, I. & Mycielski, J. (1975). J. Commun. Math. Phys. 1975, 44, 129-132.

Borgoo, A.; Jaque, P. ; Toro-Labbé, A.; Van Alsenoy, C. & Geerlings, P. (2009). Phys. Chem. Chem. Phys., 2009, 11, 76–482

Bradforth, S.E.; Arnold, D.W.; Newmark, D.M. & Manolopoulos, D.E. (1993). J Chem Phys 1993, 99, 6345-6359.

Bruhn, G. ; Davidson, E. R.; Mayer, I. & Clark, A. E. (2006). Löwdin population analysis with and without rotational invariance, Int. J. Quantum Chem. 106 (2006) 2065-2072.

Carrera, E. M. ; Flores-Gallegos, N. & Esquivel , R.O. (2010). Natural Atomic Probabilities in Quantum Information Theory , J Comp. Appl. Math. 233, 1483-1490 (2010).

Chandra, A.K. & Sreedhara-Rao, V. (1996). Int. J. Quantum Chem. 58 (1996) 57.
Chandra, A.K. (1999). Proc. Indian Acad. Sci. (Chem. Sci.) III (1999) 589.
Chattaraj, P.K.; Sarkar, U. & Roy, D. R. (2006). Chem Rev 2006, 106, 2065-2091.
Chatzisavvas, K. Ch.; Moustakidis, Ch. C. & Panos C. P. (2005) J. Chem. Phys. 2005, 123, 174111-174300.
Cerf N. J. & Adami C. (1977). Phys Rev Lett 1997,79, 5194
Coulson, C.A. (1991). "Valence", 2nd. ed., Clarendon, Oxford, 1961
Davidson, E.R. (1967). Electronic Population Analysis of Molecular Wavefunctions, J. Chem. Phys. 46, (1967) 3320-3324
de Gennes, P. G. & Hervet, H. (1983). Statistics of starburst polymers, J. Phys. Lett. 44, (1983) L351- L360.
De Proft, F.; Chattaraj, P. K.; Ayers, P. W.; Torrent-Sucarrat, M. ; Elango, M.; Subramanian, V.; Giri, S. & Geerlings, P. (2008). J. Chem. Theory Comput. 2008, 4, 595–602.
Dewar, M.J.S. (1984). J. Am. Chem. Soc. 106 (1984) 209.
Einstein, A.;. Podolsky B; & Rosen N. (1935). Phys. Rev. 1935, 47, 777.
Esquivel, R O.; Flores-Gallegos, N.; Iuga, C.; Carrera, E. ; Angulo, J. C. & Antolín, J. (2009). Theoretical Chemistry Accounts 124, 445–460 (2009)
Esquivel, R. O. ; Flores-Gallegos, N.; Carrera, E.; Dehesa, J.S. ; Angulo, J. C.; Antolín, J. & Soriano-Correa, C. (2009b). Molecular Simulation, Vol. 35, No. 6, May 2009, 498–511.
Esquivel, R O.; Flores-Gallegos, N.; Iuga, C.; Carrera, E. ; Angulo, J. C. & Antolín, J. (2010). Physics Letters A 374 (2010) 948–951
Esquivel, R. O.; Flores-Gallegos, N.; Carrera, E. & Soriano-Correa, C. (2010b). Journal of Nano Research Vol. 9 (2010) pp 1-15.
Esquivel, R O. ; Flores-Gallegos, N.; Dehesa, J.S.: Angulo, J. C. ; Antolín, J. & Sen, K. (2010c) J. Phys. Chem. A 2010, 114, 1906–1916
Esquivel, R.O.; Angulo, J.C.; Antolin, J.; Dehesa, J. S.; Flores-Gallegos, N. & S. Lopez-Rosa (2010d). Phys. Chem. Chem. Phys., 2010, 12, 7108–7116
Esquivel, R.O. ; Liu, S.; Angulo, J.C. ; Dehesa, J. S. ; Antolin, J. & Molina-Espíritu, M. (2011). J. Phys. Chem. A, 115 (2011) 4406-4415.
Esquivel, R. O. ; Molina-Espíritu, M.; Angulo, J. C. ; Antolín, J. ; Flores-Gallegos, N. & Dehesa, J. S. (2011b). Mol. Phys., 109 (2011), 2353–2365.
Esquivel, R.O.; Flores-Gallegos, N.; Molina-Espíritu, M.; Plastino, A.R.; Angulo, J.C.; Antolín, J. & Dehesa, J.S. (2011c). J. Phys. B: At. Mol. Opt. Phys. 44 175101 (2011)
Eyring, H. (1935). J. Chem. Phys. 1935, 3, 107-115
Fan, L & Ziegler, T. (1992). J. Am. Chem. Soc. 1992, 114, 10890-10897
Fischer, M. & Vögtle, F. (1999). Dendrimers : From Design to Application - A Progress Report, Angew. Chem., Int. Ed., 38, (1999) 884-905
Flores-Gallegos, N. & Esquivel, R. O. (2008). J. Mex. Chem. Soc., Volume 52, Issue 1, 19-30 (2008)
Fréchet, J M J & Tomalia, D A. (2001). Editors, Dendrimers and Other Dendritic Polymers, Chichester, U.K.: Wiley; 2001.
Fréchet, J. M. (2002). Dendrimers and supramolecular chemistry, J. Proc. Natl. U.S.A. 99, (2002) 4782-4787.
Frenkel, D.; Smit, B. , Understanding Molecular Simulation, Academic Press, San Diego, 1996.
Fukui, K. (1981). Acc. Chem. Res. 1981, 14, 363-368.
Frisch MJ; Trucks GW; Schlegel HB; Scuseria GE; Robb MA; Cheeseman JR; Montgomery Jr. JA; Vreven T; Kudin KN; Burant JC; Millam JM; Iyengar SS; Tomasi J; Barone V; Mennucci B; Cossi M; Scalmani G; Rega N; Petersson GA; Nakatsuji H; Hada M; Ehara M; Toyota K; Fukuda R; Hasegawa J; Ishida, M; Nakajima T; Honda Y; Kitao

O; Nakai H; Klene M; Li X; Knox JE; Hratchian HP; Cross JB; Bakken V; Adamo C; Jaramillo J; Gomperts R; Stratmann RE; Yazyev O; Austin AJ; Cammi R; Pomelli C; Ochterski JW; Ayala PY; Morokuma K; Voth GA; Salvador P; Dannenberg JJ; Zakrzewski VG; Dapprich S; Daniels AD; Strain MC; Farkas O; Malick DK; Rabuck AD; Raghavachari K; Foresman JB; Ortiz JV; Cui Q; Baboul AG; Clifford S; Cioslowski J; Stefanov BB; Liu G; Liashenko A; Piskorz P; Komaromi I; Martin RL; Fox DJ; Keith T; Al-Laham MA; Peng CY; Nanayakkara A; Challacombe M; Gill PMW; Johnson B; Chen W; Wong MW; Gonzalez C; Pople JA (2004). Gaussian 03, Revision D.01, Gaussian, Inc., Wallingford CT)

Gadre, S.R. (2003). Reviews of Modern Quantum Chemistry: A Celebration of the Contributions of Robert G. Parr, Vol. 1, p. 108-147, Ed. K. D. Sen, World Scientific, Singapore (2003)

Ghanty, T. K. & Ghosh, S. K. (1993). J. Phys. Chem. 1993, 97, 4951-4953

Ghosh, S. K.; M. Berkowitz & Parr, R. G. (1984). Proc. Natl. Acad. Sci. U.S.A. 1984, 81, 8028-8031

Glukhovtsev, M.N.; Pross, A. & Radom, L. (1995). J. Am. Chem. Soc. 1995, 117, 2024-2032

González, C. & Schlegel, H. B. (1990). J. Phys. Chem. 1990, 94, 5523-5527

González, C. & Schlegel, H. B. (1989). J. Phys. Chem. 1989, 90, 2154-2161

González-García, N.; Pu, J.; González-Lafont, A.; Lluch, J.M. & Truhlar, D.G. (2006). J. Chem. Theory Comput. 2006, 2, 895-904

Guevara, N. L.; Sagar, R. P. & Esquivel, R. O. (2005) J. Chem. Phys. 2005, 122, 084101

Hecht, S. & Fréchet, J M. (2001). Dendritic Encapsulation of Function: Applying Nature's Site Isolation Principle from Biomimetics to Materials Science, J. Angew Chem Int Ed Engl. 2001;40:74–91

Holister, P.; Roman-Vas, C. & Harper, T. (2003). Dendrimers, Technology White Papers", Vol 6, (2003), 1-15.

Ho, M.; Schmider, Weaver, D. F.; Smith, Jr. V. H.; Sagar, R. P. & Esquivel, R.O. (2000) Int. J Quant. Chem. 2000, 77, 376-382

Hammond, G. S. (1955). J. Am. Chem. Soc. 1955, 77, 334-338

Hati, S. & Datta, D. (1994) J. Phys. Chem. 1994, 98, 10451-10454.

Hirshfeld F. L. (1977). Theor. Chim. Acta 44, 129 (1977).

Hoffman, R.; Shaik, S. & Hiberty, P.C. (2003). Acc. Chem. Res. 2003, 36, 750-756

Ishida, K.; Morokuma, K. & Komornicki, A. (1977). J. Chem. Phys 1977, 66, 2153-2156

Janak, J. F. (1978)Phys. Rev B, 1978, 18, 7165-7168.

Jaque P.; Toro-Labbé A.; Geerlings P. & De Proft F. (2009). J. Phys. Chem. A 2009, 113, 332-344.

Jockush, S.; Ramirez, J.; Sanghvi, K. ; Nociti, R.; Turro, N. J. & Tomalia, D. A. (1999). Comparison of Nitrogen Core and Ethylenediamine Core Starburst Dendrimers through Photochemical and Spectroscopic Probes, Macromolecules 32, (1999) 4419-4423.

Johnson, B.A.; Gonzales, C.A.; Gill, P.M.W. & Pople, J.A. (1994). Chem. Phys. Lett 1994, 221, l00-108

Karafiloglou, P. & Panos, C.P. (2004) Chem. Phys. Lett. 2004, 389, 400-404

Knoerr, E.H. & Eberhart M.E. (2001). J. Phys. Chem. A 2001, 105, 880-884

Koga, T. & Morita, M. (1983). J. Chem. Phys. 1983, 79, 1933-1938

Kohout M. (2007). Program DGRID, version 4.2. 2007

Koopmans, T. A. (1933). Physica 1933, 1, 104-113

Kullback, S. & Leibler R. A. (1951). On Information and Sufficiency, Ann. Math. Stat. 1951, 22, 79-86.

Leffler, J. E. (1953). Science 1953, 117, 340-341.

Lescanec, R. L. & Muthukumar, M. (1990). Configurational characteristics and scaling behavior of starburst molecules: a computational study, Macromolecules 23, (1990) 2280 – 2288.

Liu, S. (2007). J. Chem. Phys. 2007, 126, 191107-(1-3).

Liu, L. & Breslow, R. (2003). J. Am. Chem. Soc. 125, (2003)12110.
López-Rosa, S.; Esquivel, R. O. ; Angulo, J. C. ; Antolin, J.; Dehesa, J. S. & Flores-Gallegos, N. (2010). J. Chem. Theory Comput. 2010, 6, 145–154
Löwdin, P.O. (1970). On the orthogonality problem, Adv. Quantum Chem. 5, (1970) 185
Maiti, P.K. ; Cagin, T ; Wang, G. & Goddard III, W.A. (2004). Structure of PAMAM Dendrimers: Generations 1 through 11, Macromolecules 37, (2004) 6236-6254
Martyusheva, L.M. & Seleznev, V.D. (2006) Phys. Rep. 2006, 426, 1 – 45
Massen, S. E. & Panos, C. P. (1998). Phys. Lett. A 1998, 246, 530-533
Murray J.S.; Toro-Labbé A.; Clark T. & Politzer P. (2009). J. Mol. Model. 2009, 15, 701-706
Nagy, A. (2003) J. Chem. Phys. 2003, 119, 9401-9405
Nagy, A. (2006). Chem. Phys. Lett. 2006, 425, 154-156
Nalewajski, R. F. & Parr, R. G. (2001) J. Phys. Chem. A 2001, 105, 7391-7400.
Nalewajski, R.F. (2003). Chem. Phys. Lett. 2003, 372, 28
Newkome, G. R. ; Moorefield, C. N. & Vögtle, F. (1996). Dendritic molecules: Concepts, Synthesis, Perspectives, Wiley-VCH, Weinheim, 1996
Newkome, G. R.; Moorefield, C. & Vogtle, F. (2001). Dendrimers and Dendrons, Wiley-VCH, New York, 2001
Parr, R.G.; Ayers, P.W. & Nalewajski , R. F. (2005). J. Phys. Chem. A 2005, 109, 3957-3959
Parr, R. G. & Pearson, R. G. (1983) J Am Chem Soc 105, (1983) 7512-7516
Parr, R. G. & Yang, W. (1989) "Density-Functional Theory of Atoms and Molecules", Oxford University Press: New York, 1989
Pearson, R. G. (1963). Hard and Soft Acids and Bases. J. Am. Chem. Soc. 1963, 85, 3533
Pearson, R. G. (1973) Hard and Soft Acids and Bases; Dowen, Hutchinson and Ross: Stroudsberg, 1973
Pearson, R. G. (1997). Chemical Hardness; Wiley-VCH; New York, 1997.
Peng, Ch.; Ayala, Ph.Y.; Schlegel, H. B. & Frisch, M.J. (1996). J. Comp. Chem. 1996, 17, 49-56
Pérez-Jordá, J. M. & San-Fabián, E. (1993). Comput Phys Commun 1993, 77, 46–56
Pérez-Jordá, J. M.; Becke, A. D. & San-Fabián, E. J. Chem. Phys. 1994, 100, 6520–6534.
Polanyi J.C. & Zewail A.H. (1995). Acc. Chem. Res. 1995, 28, 119-132
Politzer, P. & Truhlar, D. G. (1981). "Chemical Applications of Atomic and Molecular Electrostatic Potentials"; Academic Press: New York, 1981
Pople, J.; Krishnan, A. R.; Schlegel, H. B. & Binkley, J. S. (1978). Int. J. Quantum Chem. 1978, 14, 545-560
Rajagopal A.K. & Rendell R.W. (2002). Phys. Rev. A 2002, 66, 022104
Raju K.B.K.; Nair P.& V. and Sen K.D. (1990). Chem. Phys. Lett. 1990, 170, 89.
Ramirez, J.C.; Perez, J.M.H.; Sagar, R.P.; Esquivel, R.O.; Ho, M. & Smith Jr., V. H. (1998). Phys. Rev. A 1998, 58, 3507-3515
Reed, A.E. & Weinhold, F. (1983). Natural bond orbital analysis of near-Hartree–Fock water dimmer, J. Chem. Phys. 78, (1983) 4066-4073
Reed, A.E. ; Weinstock, R.B & Weinhold, F. (1985) Natural population analysis J. Chem. Phys. 83, (1985) 735-746
Romera E. & Dehesa, J. S. (2004) J. Chem. Phys. 2004, 120, 8906-8912
Roy, R.; Chandra, A.K. & Pal, S. (1994). J. Phys. Chem., 1994, 98, 10447-10450
Rudnick, G. & Gaspari, G. (1986). The asphericity of random walks, J. Phys. A 4, (1986) L191-194.
Safi, B.; Choho, K. & Geerlings, P. (2001). J. Phys. Chem. A 2001, 105, 591-601
Schaftenaar G. & Noordik J.H. (2000). "MOLDEN: a pre- and post-processing program for molecular and electronic structures" J. Comput.-Aided Mol. Design 2000, 14,123-134.
Schlegel, H. B. (1987). Adv. Chem. Phys. 1987, 67, 249-286.
Schmidt, M. W.; Gordon, M.S. & Dupuis, M. (1985). J. Am. Chem. Soc. 1985, 107, 2585-2589

Sen, K. D. (2005) J. Chem. Phys. 2005, 123, 074110(1-9)
Sen K. D. & Katriel, J. (2006) J. Chem. Phys. 2006, 125, 074117-(1-4)
Shaik, S.; Ioffe, A.; Reddy, A.C. & Pross, A. (1994). J. Am. Chem. Soc. 1994, 116, 262-213
Shaik, S.S.; Schlegel, H.B. & Wolfe, S. (1992). Theoretical Aspects of Physical Organic Chemistry: The SN2 reaction, Wiley, New York, 1992.
Shannon, C.E. (1948). Bell Syst. Tech. J. 1948, 27, 379-423.
Shannon, C. E.& W. Weaver (1949), *The Mathematical Theory of Communication* (University of Illinois, Urbana, IL), (1949).
Shi, Z. & Boyd, R.J. (1991). J. Am. Chem. Soc. 1991, 113, 1072-1076.
Shi, Z. & Boyd, R.J. (1989). J. Am. Chem. Soc. 1989, 111, 1575-1579
Shi, Q. & Kais, S. (2005) J. Chem. Phys. 2005, 309, 127-131
Simon-Manso, Y. & Fuenteaelba, P. (1998) J. Phys. Chem. A 1998, 102, 2029-2032.
Tachibana, A. J. (2001). Chem. Phys. 2001, 115, 3497-3518
Tarazona-Vasquez, F. & Balbuena, P. B. (2004a). Plexation of the Lowest Generation Poly(amidoamine)-NH2 Dendrimers with Metal Ions, Metal Atoms, and Cu(II) Hydrates: An ab Initio Study, J. Phys. Chem. B 108, (2004)15992-16001
Tarazona-Vasquez, F. & Balbuena, P. B. (2004b). Ab Initio Study of the Lowest Energy Conformers and IR Spectra of Poly(amidoamine)-G0 Dendrimers J. Phys. Chem. B 108, (2004) 15982-15991
Tomalia, D. A. ; Baker, H. ; Dewald, J. ; Hall, M.; Kallos, G.; Martin, S. ; Roeck, J. ; Ryder, J. & Smith, P. (1985). A New Class of Polymers: Starburst Dendritic Macromolecules Polym. J. 17, (1985) 117-132
Tomalia, D. A. ; Naylor, A. M. & Goddard III, W. A. (1990). Starburst Dendrimers: Molecular-Level Control of Size, Shape, Surface Chemistry, Topology, and Flexibility from Atoms to Macroscopic Matter Angew. Chem.,Int. Ed. Engl., 29 (1990)138-175
Toro-Labbé, A.; Gutiérrez-Oliva, S.; Murray, J.S. & Politzer, P. (2009). J. Mol. Model., 2009, 15, 707-710
Toro-Labbé, A.; Gutiérrez-Oliva, S.; Murray, J.S. & Politzer, P. (2007). Mol. Phys., 2007, 105, 2619–2625
Tozer, D. J. & De Proft, F. (2005). J. Phys. Chem. A 2005, 109, 8923.
Vedral, V. (2002). The role of relative entropy in quantum information theory, Rev Mod. Phys. 74, (2002)197-234
Vögtle, F. ; Gestermann, S.; Hesse, R.; Schwierz, H. & Windisch, B. (2000). Prog. Polym. Sci., 25, (2000) 987.
von Neumann, J. (1955). *Mathematical Foundations of Quantum Mechanics*, 1955 translated from the German ed. by R. T. Beyer (Princeton University, Princeton).
Wehrl, A. (1978). General properties of entropy, Rev. Mod. Phys. 50, (1978) 221-260
Wigner, E. (1938). Trans. Faraday SOC. 1938, 34, 29-41.
Woodward, R.B. & Hoffmann, R. H. (1969). Angew. Chem. Int. Ed. Engl. 8 (1969) 781.
Zeng, F. & Zimmerman, S. C. (1997). Chem. Rev., 97, (1997) 1681.
Zewail, A.H. (1988). Science, 1988, 242, 1645-1653
Zewail, A.H. (1990). Sci. Am. 263 (1990) 76
Zewail, A. H. (2000a). J. Phys. Chem. A 2000, 104, 5660-5694
Zewail, A.H. (2000b) Phys. Chem. A 104 (2000) 5660-5694.

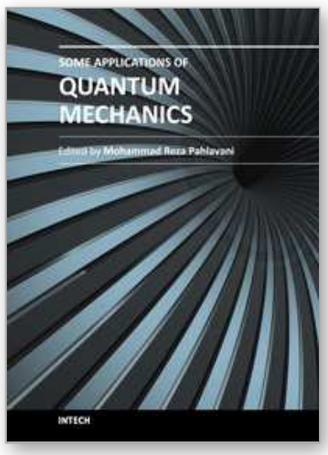

Some Applications of Quantum Mechanics

Edited by Prof. Mohammad Reza Pahlavani

ISBN 978-953-51-0059-1
Hard cover, 424 pages
Publisher InTech
Published online 22, February, 2012
Published in print edition February, 2012

Quantum mechanics, shortly after invention, obtained applications in different area of human knowledge. Perhaps, the most attractive feature of quantum mechanics is its applications in such diverse area as, astrophysics, nuclear physics, atomic and molecular spectroscopy, solid state physics and nanotechnology, crystallography, chemistry, biotechnology, information theory, electronic engineering... This book is the result of an international attempt written by invited authors from over the world to response daily growing needs in this area. We do not believe that this book can cover all area of application of quantum mechanics but wish to be a good reference for graduate students and researchers.

How to reference

In order to correctly reference this scholarly work, feel free to copy and paste the following:

Rodolfo O. Esquivel, Edmundo M. Carrera, Cristina Iuga, Moyocoyani Molina-Espíritu, Juan Carlos Angulo, Jesús S. Dehesa, Sheila López-Rosa, Juan Antolín and Catalina Soriano-Correa (2012). Quantum Information-Theoretical Analyses of Systems and Processes of Chemical and Nanotechnological Interest, Some Applications of Quantum Mechanics, Prof. Mohammad Reza Pahlavani (Ed.), ISBN: 978-953-51-0059-1, InTech, Available from: http://www.intechopen.com/books/some-applications-of-quantum-mechanics/quantum-information-theoretical-analyses-of-systems-and-processes-of-chemical-and-nanotechnological-

INTECH
open science | open minds

InTech Europe
University Campus STeP Ri
Slavka Krautzeka 83/A
51000 Rijeka, Croatia
Phone: +385 (51) 770 447
Fax: +385 (51) 686 166
www.intechopen.com

InTech China
Unit 405, Office Block, Hotel Equatorial Shanghai
No.65, Yan An Road (West), Shanghai, 200040, China
中国上海市延安西路65号上海国际贵都大饭店办公楼405单元
Phone: +86-21-62489820
Fax: +86-21-62489821

© 2012 The Author(s). Licensee IntechOpen. This is an open access article distributed under the terms of the Creative Commons Attribution 3.0 License, which permits unrestricted use, distribution, and reproduction in any medium, provided the original work is properly cited.

IntechOpen

IntechOpen